Use of Shear Wave Velocity for Foundation Design

Harry George Poulos (harry.poulos@coffey.com)
Tetra Tech Coffey

Research Article

Keywords: Correlations, empirical method, foundation design, geophysics, load-settlement, pile foundation, shallow foundation.

Posted Date: May 28th, 2021

DOI: https://doi.org/10.21203/rs.3.rs-493427/v1

USE OF SHEAR WAVE VELOCITY FOR FOUNDATION DESIGN

Harry G Poulos

Tetra Tech Coffey, Sydney, Australia

ABSTRACT

This paper describes an approach for utilizing in-situ measurements of shear wave velocity Vs to carry out preliminary and check design calculations for shallow and deep foundations. For estimates of foundation movements, Vs can be used directly to estimate the small-strain stiffness of the soil or rock strata, while for ultimate capacity calculations, use is made of empirical correlations between Vs and penetration resistance measures, which in turn are correlated to the foundation resistance characteristics. The approach is applied to a series of published tests on shallow footings, and on a series of pile load tests for a very tall building. For these cases, comparisons of the calculated with the measured load – settlement behaviour indicates that the suggested approach provides a reasonable, albeit somewhat conservative, level of agreement.

KEY WORDS

Correlations; empirical method; foundation design; geophysics; load-settlement; pile foundation; shallow foundation.

INTRODUCTION

Modern foundation design frequently involves the use of advanced numerical methods and software, which, in principle, enables more accurate calculations to be made of the anticipated behaviour of the foundation in question. However, elements of uncertainty persist, including the difficulty of characterizing and quantifying the ground conditions, and the inherent dangers of the complex software being utilized by relatively inexperienced designers. Thus, it may be advantageous to make use of various measures of the ground behaviour in developing designs, and also of having simpler methods of checking the validity and reasonableness of the design outcomes from complex software.

This paper sets out an approach that utilizes in-situ measurements of shear wave velocity in conjunction with empirical correlations of geotechnical design parameters. The shear wave velocity provides a direct measurement of the small-strain stiffness of soil and rock strata, and corrections can then be made to allow for larger levels of strain likely to occur due to foundation loading. The empirical correlations are used to estimate alternative parameters (SPT and CPT) from which design parameters for the capacity of shallow and deep foundations can be estimated.

The approach developed is applied to published load tests for a series of shallow footings on sand, and a series of pile load tests in soft calcareous rocks.

ASSESSMENT OF SHEAR WAVE VELOCITY, V_s

Direct In-Situ Measurements

Geophysical methods have been used increasingly over the past few decades as part of geotechnical site investigations. These methods are generally non-invasive or minimally invasive, and can provide extremely valuable additional data to conventional site investigation techniques which may involve

borehole drilling and sampling, various forms of penetration testing, and testing involving pressuremeter or dilatometer. A committee of the Deep Foundation Institute (DFI) has examined various aspects of geophysical testing, and has concluded that "Through the early incorporation of geophysics into the project team and better communication between all team members, the successful application of geophysics throughout geotechnical investigations can be expanded" (Garfield et al, 2021).

Of particular relevance to foundation engineering is the shear wave velocity, V_s, which can be related directly to the in-situ stiffness of the ground through which the shear waves travel. V_s can be measured directly via in-situ geophysical methods, for example, as described by Godlewski and Szczezepanski (2015). They identify three broad approaches to in-situ measurement:

1. Via surface waves, using techniques such as Multi-channel Analysis of Surface Waves (MASW), Spectral Analysis of Surface Waves (SASW) and Continuous Surface Wave System (CSWS);
2. Via boreholes, using down-hole, cross-hole or up-hole techniques, or P-S suspension logging;
3. Via soundings, such as the seismic CPT (cone penetrometer test) or the seismic DMT (dilatometer) test.

Surface wave methods are non-invasive, while downhole, cross-hole and up-hole methods all require at least one borehole to be drilled into the material, with the hole being appropriately prepared with PVC casing and grouting around the annulus. While non-invasive testing eliminates the need for penetration into the subsurface, it also does not allow for physical sampling of the material. Moreover, cross-hole techniques are likely to be the most reliable indicators of the variability of V_s with depth. However, very accurate 3-dimensional positioning is required if the holes are closely spaced, and it may be necessary to use an additional borehole deviation tool when the holes are non-vertical.

Traditionally, the geophysical industry has made almost exclusive use of P waves, but in relatively soft saturated soils, the P-wave velocity is dominated by the bulk modulus of the pore fluid. If the ground is saturated, and the skeleton relatively compressible, the P-wave velocity will not be much different from that of water (about 1500 m/s*).* Therefore it is not possible to distinguish between different soil or rock properties on the basis of P-wave velocities until the bulk modulus of the skeleton of the soil or rock is substantially greater than that of water. Thus, for soils and soft rocks, the shear wave velocity will be the quantity that will be of most general use.

In-situ measurements of shear wave velocity, V_s, have a major advantage over laboratory measurements in that the effects of geological features such as jointing, faulting and weathering, are reflected in a reduction in V_s as compared with values within a homogeneous sample or mass. Thus, some corrections that need to be made to laboratory-measured parameters, such as those for rock mass quality, are no longer necessary if in-situ measurements of V_s are made and the design parameters are then derived from those V_s values.

Correlations of Shear Wave Velocity with In-Situ Stress State and Soil Compressibility

In cases where SPT or CPT data are not available, it is also possible to estimate V_s from the in-situ stress state and the compressibility of the soil.

Cha et al (2014) have examined correlations between the compressibility of soils (compression Index, C_c) and shear wave velocity V_s. They first relate V_s to the effective stresses in the direction of particle motion and the direction of wave propagation, σ'_p and σ'_w respectively (in kPa), as follows:

$$Vs = \alpha.[(\sigma'_p + \sigma'_w)/2]^{\beta} \quad \text{(kPa)} \qquad (1)$$

From experimental data, they then relate the parameters α and β to the compression index C_c, giving

$$\alpha = 13.5.C_c^{-0.063} \text{ (m/s)} \quad (2)$$

and $$\beta = 0.17.C_c + 0.43 \quad (3)$$

and thus,

$$\beta = 0.73 - 0.27.\log(\alpha), \quad \text{for } 1 \leq \alpha \leq 500 \text{ m/s}. \quad (4)$$

Typical Values of V_s

As a very rough guide, typical values of V_s for various geo-materials, and for concrete, are shown in Table 1.

Table 1: Typical Values of V_s for Various Materials

Material	*Shear wave velocity V_s m/s*
Very soft soil	85-105
Soft soil	106-135
Medium soil	136-185
Stiff soil	186-275
Very stiff soil	276-365
Soft rock/cemented soil	366-760
Rock	761-1500
Hard rock	>1500
Concrete	2286-2438

It should be emphasized that significant variability in measured values of V_s can occur in a single geologic unit. In rocks, factors such as weathering and the presence of discontinuities can have a significant impact on the V_s of rocks. Rocks such as limestone can exhibit profound variations in V_s, largely as a function of weathering, and depending on site conditions, an order of magnitude change in V_s can occur over a relatively short distance.

Relationship Between Shear (S-) Wave and P-Wave Velocities

In some cases, especially in relation to rocks, values of the compressional P-wave velocity, V_p, may be available rather than values of shear (S-wave) velocity, V_s. Theoretically, for an ideal homogeneous elastic mass, V_p and V_s are related via the following expression:

$$V_p = V_s [2/(1-2\nu) + 1]^{0.5} \quad (5)$$

where ν = Poisson's ratio.

The relationship between the ratio V_p / V_s and ν is shown in Figure 1. For a typical value of $\nu = 0.25$ for rock, $V_p/V_s = 2.24$.

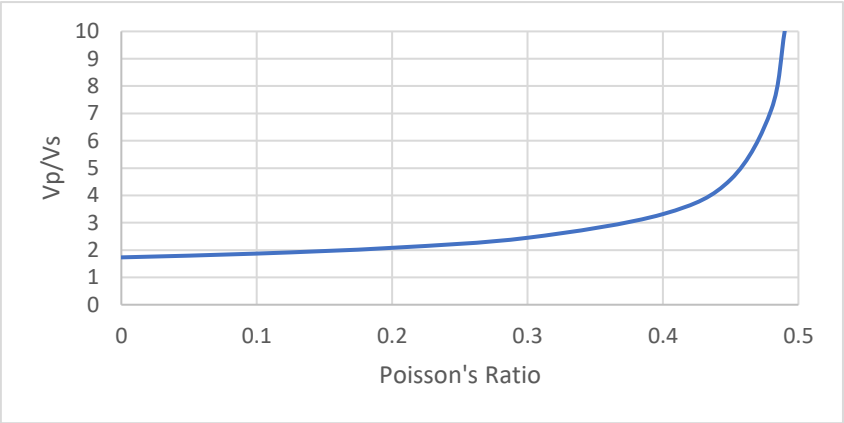

Figure 1: Theoretical relationship between V_p/V_s and Poisson's ratio ν

CORRELATIONS BETWEEN WAVE VELOCITIES AND STIFFNESS AND STRENGTH PARAMETERS

Soil Stiffness

A rigorous relationship exists between V_s and the small strain shear modulus, G_0, of a material, namely:

$$G_0 = \rho . V_s^2 \quad (6)$$

where ρ = mass density of the material, and V_s = shear wave velocity.

The Young's modulus for small strain, E_0, is then

$$E_0 = 2(1+\nu).G_0 \quad (7)$$

where ν = Poisson's ratio of the material.

For design purposes, these values can be used, with modification, to estimate foundation movements, as discussed later in this paper.

Soil Strength

Rigorous relationships between V_s and strength properties for soils do not exist, and so resort must be made to empirical correlations.

For clay soils, L'Heureux and Long (2017) have reviewed a number of published correlations between V_s and undrained shear strength s_u. Three of these have been evaluated and summarized in Figure 2. There is a very wide dispersion of values of s_u, and it appears that such correlations are unlikely to give reliable indications of undrained shear strength of clays. However, the correlations of Agaiby and Mayne (2015) and L'Heureux and Long (2017) appear to be reasonably consistent and provide intuitively reasonable values of s_u. The corresponding correlations are as follows:

Agaiby and Mayne (2015): $s_u = 0.152.V_s^{1.142}$ (8)

L'Heureux and Long (2017): $s_u = 0.02.V_s^{1.45}$ (9)

where V_s is in m/s and s_u is in kPa.

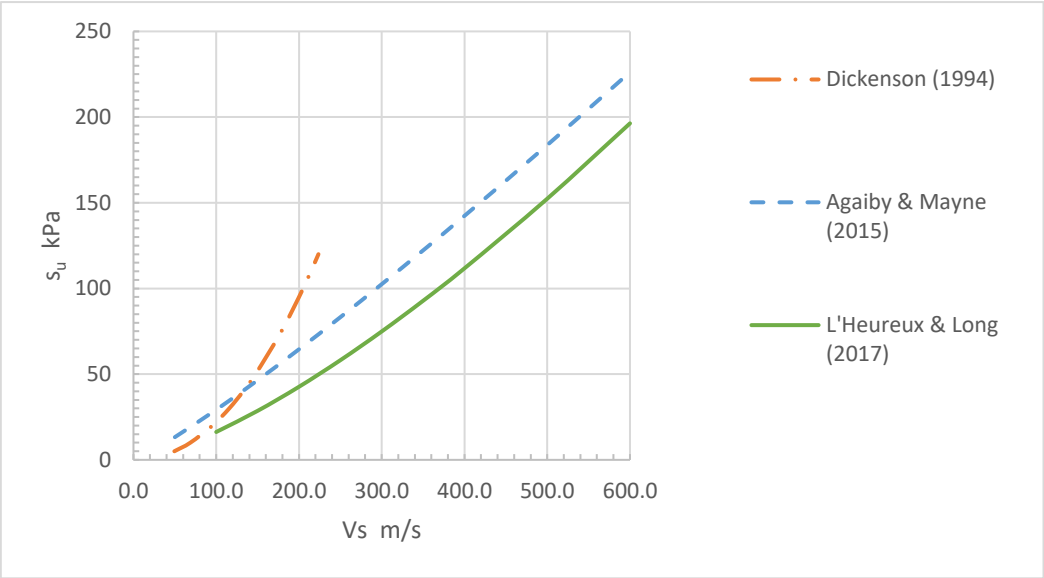

Figure 2: Correlations of s_u versus V_s

For coarse-grained soils, correlations for the conventional strength parameters, angle of internal friction (and cohesion if the soil is cemented) are not usually relied upon, and so indirect correlations with more readily-measured characteristics such as SPT or CPT resistances are normally exploited. Such correlations are discussed further later in the paper.

Correlations for Rocks

Many of the available correlations for rock strength relate the unconfined compressive strength, UCS, with the P-wave velocity, V_p, for example, Azimian et al (2014), Majstorovic et al (2014). Cheenikal et al (2007) have suggested the broad correlations shown in Table 2, while a summary of some published correlations for various rock types have been provided by Altindag (2012). These are reproduced in Table 3, and the correlations shown are those which have a power law that does not give negative values of UCS. It can be observed that the correlations in this table are for relatively hard rocks, and there appear to be no corresponding correlations for soft rocks.

Table 2: Correlations between P-wave velocity and UCS (Cheenikal et al, 2007)

Seismic Velocity V_p (km/s)	*Geotechnical Description*	*UCS (MPa)*
<2.0	Low strength rock	<10
2.0 – 2.5	Medium strength rock	10 - 20
2.5 – 3.5	High strength rock; stratified, jointed	20 - 60
3.5 – 7.0	Very high strength rock	> 60

Table 3: Some correlations between V_p and UCS (after Altindag (2013)

Equation Number	*Correlation*	*Rock type*
1	UCS = 0.78 $V_p^{0.88}$	Volcanic group
2	UCS = 9.95$V_p^{1.21}$	Marl, limestone, dolomite, sandstone, hematite, serpentine, diabase, tuff

3	UCS = 22.03 $V_p^{1.247}$	Granites
4	UCS = 2.304 $V_p^{2.4315}$	Diorite, quartzite, sandstone, limestone, marble, granodiorite, basalt, travertine, trachyte, tuff, andesite
5	UCS = 12.746 $V_p^{1.194}$	Limestone, sandstone, travertine, marl, dolomite, mudrock-shale, slate, siltstone

Note: UCS in MPa, V_p in km/s

Based on a very limited amount of data, with considerable scatter of results, at the site of the Burj Khalifa (Hyder, 2004), for shear wave velocities up to about 1.30 km/s, the author has developed the following very rough correlation for weakly cemented calcareous sands and weak carbonate rocks:

$$UCS \approx 3.5V_s \quad MPa \qquad (10)$$

where V_s is in km/s

If V_p is converted to V_s via the relationship in equation (5), then for a typical Poisson's ratio of 0.25, Figure 3 plots the correlations between UCS and V_s from the correlations in Table 2 (simplified to a continuous curve), together with that in equation (10). It can be seen that the correlations are widely dispersed, indicating that they are highly dependent on the rock type and its geological origin. Equations 2, 3 and 5 in Table 3 appear to be relevant to hard rocks, while equation 1 and the very rough correlations suggested herein in equation 10 appear to be more relevant to softer rocks.

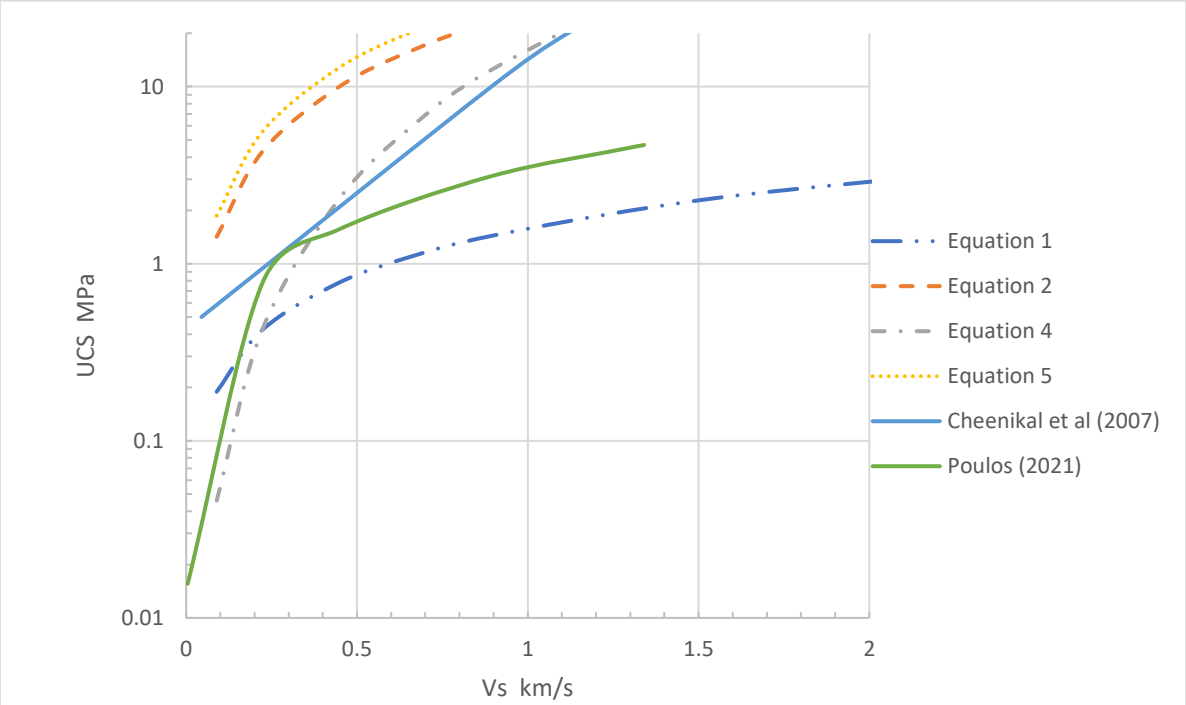

Figure 3: Some relationship between UCS and V_s (V_s derived from V_p)

DERIVATION OF SHALLOW FOUNDATION DESIGN PARAMETERS

Ultimate Limit State Parameters

Via SPT Correlations

There are very few direct correlations between shear wave velocity V_s and foundation design parameters, and so from a practical viewpoint, one of the approaches that can be adopted is to relate V_s to other in-situ measurements for which correlations exist. The most obvious, but probably most variable, correlations are with the SPT-N value, and such correlations often take the following form:

$$V_s = A.N^B \quad (11)$$

where A, B are empirical parameters, and N = measured SPT value.

There is a very wide spread of suggested values of A and B, and some of these values are shown in Table 4.

Table 4: Correlation factors A and B

Soil Type	*A*	*B*	*Source*
All types	97	0.314	Imai and Tonouchi (1982)
Fine-grained	100	0.33	JRA (1980)
Coarse-grained	56	0.5	Seed et al (1983)

Some correlations have incorporated the effect of the vertical effective stress σ_v', giving a relationship of the following form:

$$V_s = a.N_{60}\ b.(\sigma_v')^c \quad (12)$$

where a, b and c are empirical parameters, and N_{60} is the SPT value corrected for a 60% energy ratio.

Wair et al (2012) present values of a, b and c from various sources, but in many cases, it may be debatable whether the additional refinement is justifiable.

Using the simpler expression in equation (11), the equivalent SPT value, N_e, can then be derived from V_s as:

$$N_e = (V_s/A)^{1/B} \quad (13)$$

For ultimate limit state calculations, use can then be made of correlations between ultimate bearing capacity p_u and SPT. For example, Decourt (1995) provides the following approximation for shallow foundations:

$$p_u = K.N_e \text{ kPa} \quad (14)$$

where K = 90 for sands, 80 for intermediate soils and 65 for saturated clays.

It must be recognized that this approach may be very approximate, as it makes use of one correlation upon another, but at least it may provide an estimate of the order of magnitude of p_u.

Via Correlations with CPT

Among the many published correlations between V_s and static cone (CPT) resistance, q_c, are those of Hegazy and Mayne (1995), which are of the following form:

$$V_s = F1.q_c^{F2}.f_s^{F3} \quad m/s \tag{15}$$

where q_c = measured cone resistance in kPa, f_s = measured cone sleeve resistance, in kPa, and F1, F2 and F3 are empirical parameters, as shown in Table 5.

Table 5: Empirical parameters F1, F2 and F3 (Hegazy and Mayne, 1995)

Soil Type	*F1*	*F2*	*F3*
Sand	13.18	0.192	0.179
Clay	3.18	0.549	0.025

From equation (15), the corresponding equivalent value of q_c, q_{ce}, can be roughly estimated as follows:

$$q_{ce} = [V_s/(F1.f_s^{F3})]^{1/F2} \tag{16}$$

Using this derived value of q_{ce}, the ultimate bearing capacity of a shallow footing, p_u, can then be estimated from correlations such as those in MELT (1993), as follows:

$$p_u = a_1[1 + a_2.D/B]\, q_{ce} + q_0 \tag{17}$$

where a_1, a_2 are parameters depending on soil type and condition (Table 6)

q_0 = overburden pressure at level of base.

q_c = cone tip resistance.

D = depth of embedment below surface.

B = average width of footing.

Table 6: Parameters a_1 and a_2 for Ultimate Bearing Capacity of Square Shallow Footings and Rafts (after MELT, 1993)

Soil Type	*Condition*	*a_1*	*a_2*
Clay, silt	All	0.32	0.35
Sand, gravel	Loose	0.14	0.35
	Medium	0.11	0.50
	Dense	0.08	0.85
Chalk	-	0.17	0.27

Other correlations of pile shaft friction and end bearing with CPT are summarised and critically reviewed by Niazi and Mayne (2013).

For Rocks

As a first approximation, the ultimate bearing capacity for shallow foundations on rock, p_u, can be estimated, conservatively, as:

$$p_u = A1(UCS)^{A2} \text{ MPa} \quad (18)$$

where UCS = unconfined compressive strength, in MPa, and A1, A2 are empirical parameters. Typically, it is reasonable to adopt A1 = 3 and A2 = 0.5 for preliminary design.

Serviceability Limit State Parameters

If an elastic-based approach is used to estimate foundation movements, a value of Young's modulus, E_s, or shear modulus, G_s, is required. Small-strain values of these moduli can be derived from V_s via equations 7 and 6 respectively. However, when applying these to the estimation of foundation movements at normal serviceability load levels, the small-strain values must be reduced to take account of the larger strains within the soil. An approximate, but very convenient, way of making these reductions is that proposed by Mayne (2001), based on work by Fahey and Carter (1993). Via Mayne's approach, the reduction factor, R_E, to be applied to the small strain modulus values can be expressed as follows:

$$R_E = 1\text{-}f.(p/p_u)^g \quad (19)$$

where p = average applied pressure, p_u = ultimate bearing pressure, and f and g are experimentally-obtained parameters. Mayne quotes typical values as f = 1 and g = 0.3.

When using an approach that does not explicitly allow for an increase in stiffness with increasing depth below the footing, use can be made of approximate calculations using the Boussinesq theory to compute the distribution of vertical stress with depth, and then to derive a relationship between the ratio of the modulus to the small-strain modulus, as a function of the relative depth below the foundation, and the applied stress level relative to the ultimate bearing capacity p_u. Such a relationship is shown in Figure 4 for a uniformly loaded circular footing of diameter d, and can be used as a convenient, albeit approximate, means of estimating the distribution of modulus with depth below the footing. The settlement, S, can then be calculated by computing the vertical strain at various levels from the computed stress increases and the modulus values at those corresponding levels, i.e.

$$S = \sum \{(d\sigma_{zi} - 2\nu.d\sigma_{ri})*h_i)/\{E_{oi}.(E/Eo)\} \quad (20)$$

where $d\sigma_{zi}$, $d\sigma_{ri}$ = vertical and radial stress increments within a sub-layer at an average depth z_i below the surface, h_i = thickness of sub-layer i, E_{oi} is the small-strain Young's modulus of sub-layer i, and E/Eo = the ratio of modulus to small-strain modulus in sub-layer i, as plotted in Figure 4.

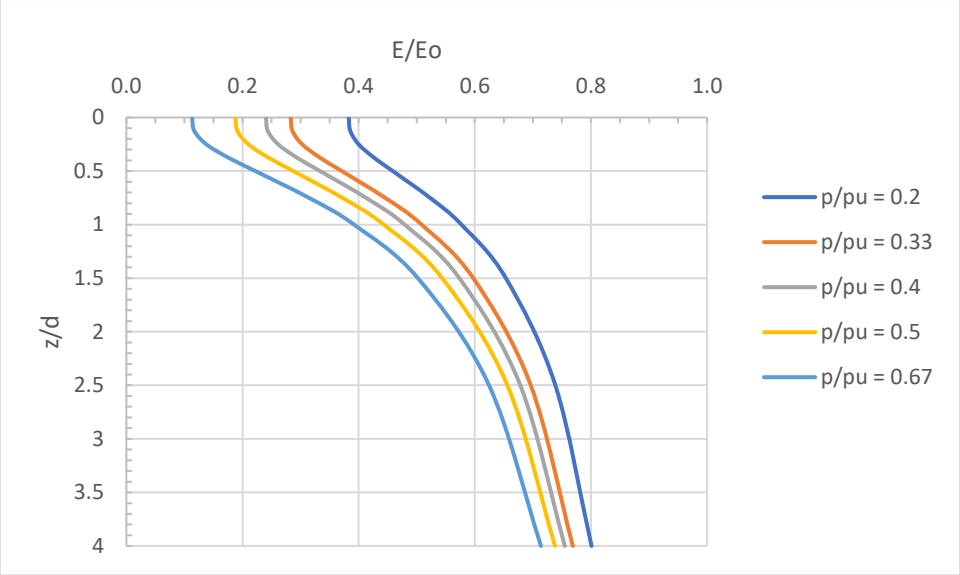

Figure 4: Modulus reduction factors for a shallow circular footing.

z = depth below surface, d = equivalent footing diameter, p/p_u = average pressure divided by ultimate value, E/E_o = modulus relative to small-strain value.

APPLICATION TO SHALLOW FOOTING TESTS

The approach developed above has been applied to the shallow footing tests on sand reported by Briaud and Gibbens (1994). Five spread footings located on a sand site were tested to failure, and predictions made by various people of the load-settlement characteristics of these footings were presented. A variety of in-situ and laboratory test data was available for the site, including SPT data, CPT data, pressuremeter tests, dilatometer tests, borehole shear tests, step blade tests, and cross-hole wave tests. Here, the measured shear wave velocities from the cross-hole tests have been used to try and predict the settlement and vertical load capacity of the footings.

Shear wave tests were carried out in two orthogonal directions, and the results are shown in Table 7. From these tests, values of the equivalent SPT value, Ne, were derived using the relationship of Seed et al (1983), and an average value of Ne was adopted, as shown in Table 7. It should be noted that an alternative Vs-N correlation of Imai and Tonouchi (1978) gave reasonably similar results for Ne to that from the Seed et al correlation.

Table 7: Measured values of Vs and derived values of average Ne

Depth m	*Vs (N-S) m/s*	*Vs (E-W) m/s*	*Ne (N-S)*	*Ne (E-W)*	*Average Ne*
2	240	202	18	13	15.5
4	300	211	28	14	21
6	281	210	25	14	19.5
8	199	170	12	9	10.5
10	238	230	18	17	17.5

Figure 5 compares the derived average values of Ne with those actually measured (from Table 9 of Briaud and Gibbens, 1994). There is a reasonable correspondence between the measured and derived values of SPT-N within the upper 10 m in which V_s values were measured.

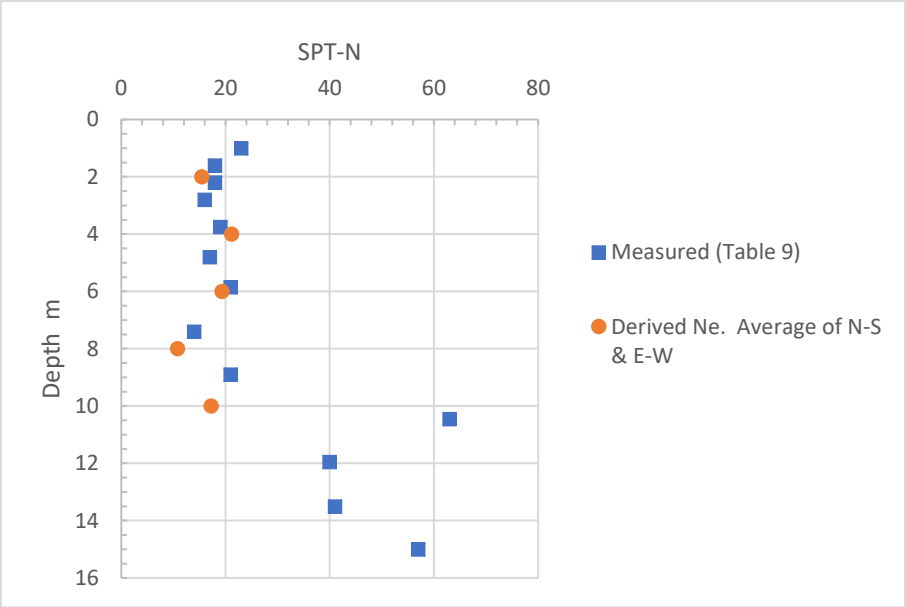

Figure 5: Comparison between measured and derived SPT values

The following approach was adopted herein in calculating the load-settlement behaviour of the footings:

1. The soil profile was divided into a series of sub-layers, ranging in thickness from 0.2 m within the upper 1 m of the soil profile to 1 m at depths below 5 m. A total of 16 sub-layers were used.
2. The equivalent SPT values, Ne, within each sub-layer were used to estimate the small-strain Young's modulus values E_0 at the centre of each sub-layer.
3. The ultimate bearing capacity, p_u, of the footing was estimated from the Decourt expression in equation 14.
4. For increasing values of the average applied pressure p, the vertical and radial stress increments were computed from Boussinesq theory, and the ratio of footing pressure to p_u at the centre of each sub-layer was obtained.
5. From Figure 4, the ratio of Young's modulus E to small-strain Young's modulus E_0 was obtained for each sub-layer.
6. The settlement for the specified average applied pressure was calculated from equation 20.
7. Because the calculation is based on strains below the centre of a uniformly (and perfectly flexible) footing, a correction for footing rigidity was applied, as per Mayne and Poulos, 1999.
8. The calculation was repeated for increasing pressures until an applied pressure close to the ultimate value was reached.

Figures 6 to 9 show comparisons between the measured and calculated load-settlement curves for the five footings. The calculated curves tend to over-predict the settlement (except for the 3 m diameter South footing, where the agreement is remarkably close. Overall, the agreement is not unreasonable, and it would appear that the approach adopted provides an acceptably conservative design approach for shallow footings on sand.

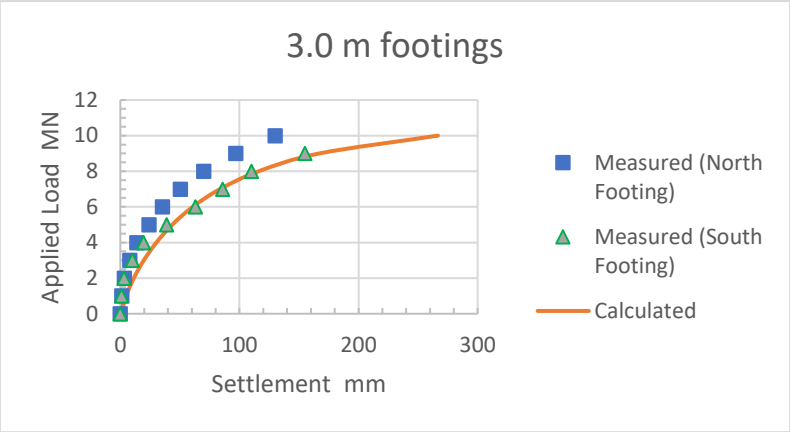

Figure 6: Measured and calculated load-settlement curves for 3 m diameter footings

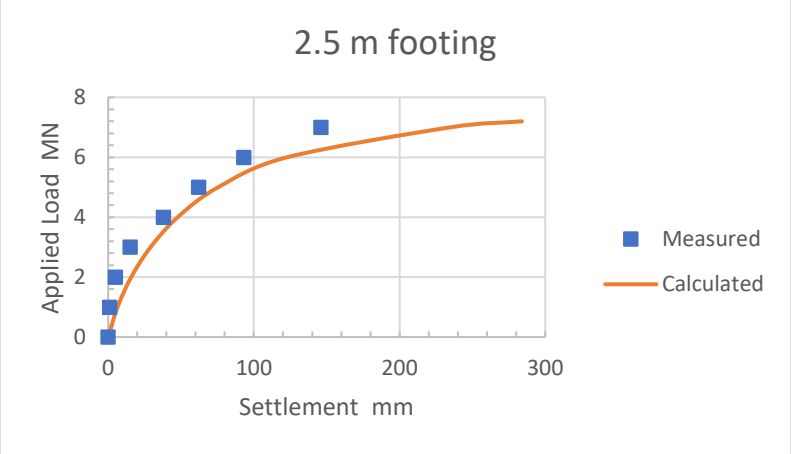

Figure 7: Measured and calculated load-settlement curves for 2.5 m diameter footing

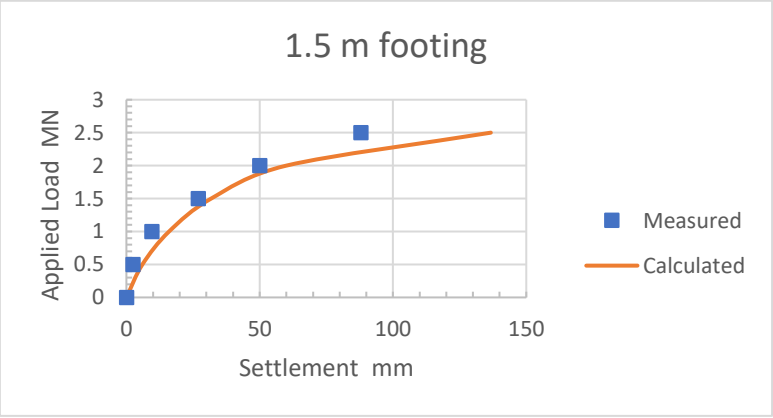

Figure 8: Measured and calculated load-settlement curves for 1.5 m diameter footing

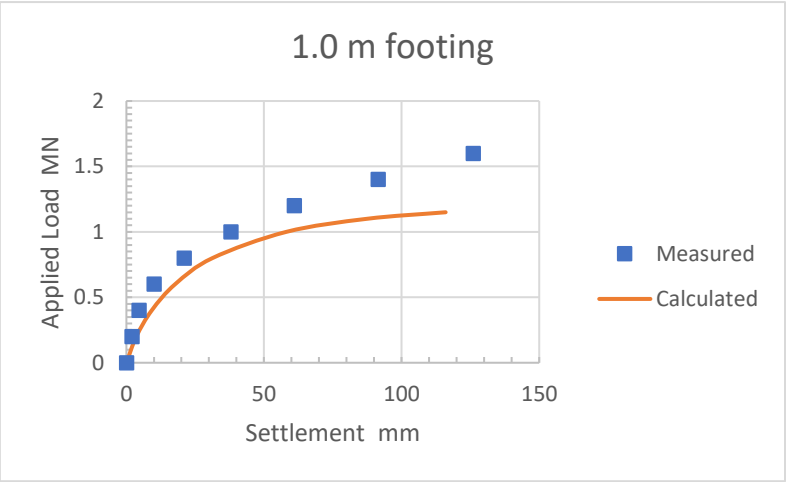

Figure 9: Measured and calculated load-settlement curves for 1 m diameter footing

DERIVATION OF DEEP FOUNDATION DESIGN PARAMETERS

Ultimate Limit State

Because of the uncertainty in correlating basic strength parameters with shear wave velocity V_s, use will be made of correlations between the deep foundation parameters for the ultimate limit state, and the equivalent SPT value, N_e, derived from correlation with V_s, as per equation 13.

(a) For Soil Strata

The following correlations between SPT and pile design parameters have been provided by Decourt (1995).

The ultimate shaft friction, f_s,

$$f_s = a(2.8N_e + 10)\ \text{kPa} \qquad (20)$$

where a = 0.6 for bored piles, and 1.0 for driven piles.

The ultimate end bearing, f_b, is approximated as:

$$f_b = K_b.N\ \text{kPa} \qquad (21)$$

where for displacement piles, K_b = 320 for sands, 205 for sandy silt, 165 for sandy silt, and 100 for clay, while for non-displacement piles, the corresponding vales are 165, 115, 100 and 80.

Using these correlations, Figures 10 to 13 below show the results of calculations based on the V_s versus SPT relationships from JRA (1980) for fine-grained soils, and Seed et al (1983) for coarse-grained soils.

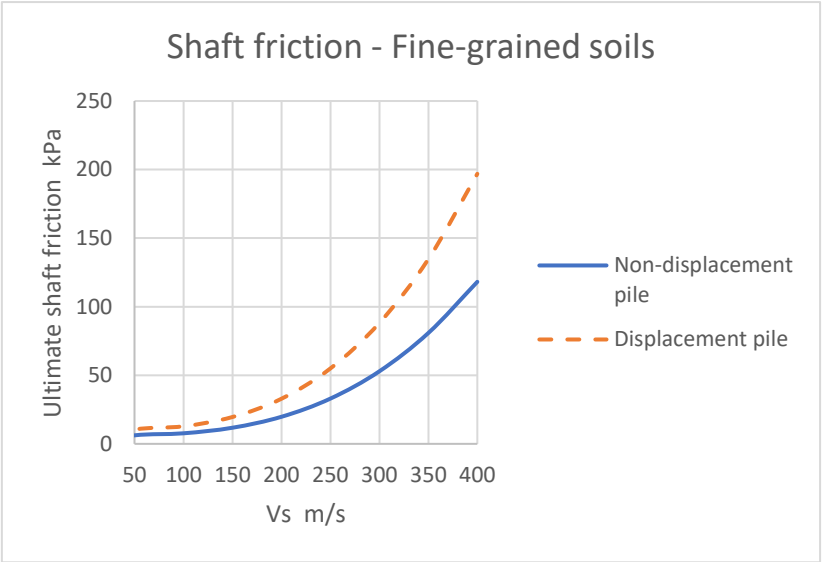

Figure 10: Approximate correlations between ultimate shaft friction and V_s for fine-grained soils

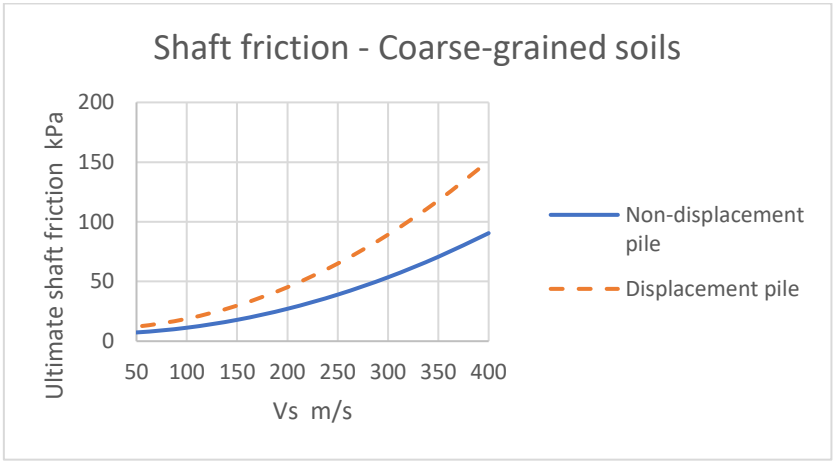

Figure 11: Approximate correlations between ultimate shaft friction and V_s for coarse-grained soils

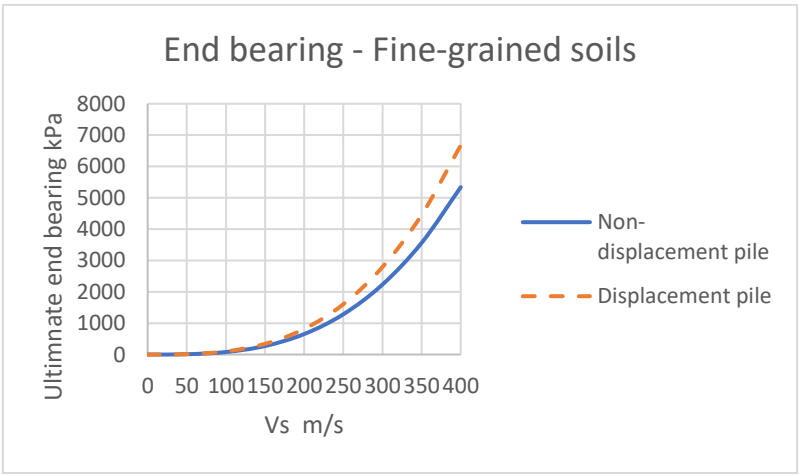

Figure 12: Approximate correlations between ultimate end bearing and V_s for fine-grained soils

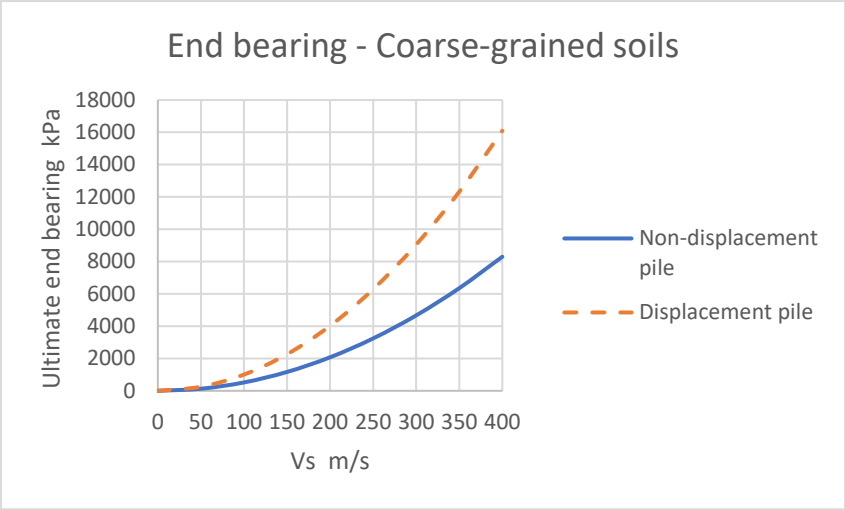

Figure 13: Approximate correlations between ultimate end bearing and V_s for coarse-grained soils

An alternative procedure can be developed using the deduced values of static cone resistance (CPT) to estimate both shaft and base ultimate resistances. Niazi and Mayne (2013) provide a very comprehensive summary of various CPT-based approaches.

(b) for Rock Strata

For pile foundations on or within rock, the following approximations can be employed:

Ultimate shaft friction: $f_s = A3(UCS)^{A4}$ MPa (22)

Ultimate end bearing: $f_b = A5(UCS)^{A6}$ MPa (23)

where UCS = unconfined compressive strength, in MPa, and A3, A4, A5 and A6 are empirical parameters.

Typically, the following relatively conservative values can be adopted for preliminary design:

A3 = 0.3, A4 = 0.5, A5 = 4.8, A6 = 0.5 (Poulos, 2017).

Serviceability Limit State Parameters

Via Mayne's approach, the reduction factor, R_E, to be applied to the small strain modulus values for an axially loaded pile or pile group can be expressed as follows:

$$R_E = 1\text{-}f(FS)^{-g} \quad (24)$$

where FS = factor of safety against failure, and f and g are experimentally-obtained parameters, typical values again being f = 1 and g = 0.3.

Figure 14 plots the reduction factor R_E against FS, and shows a very rapid reduction in R_E as FS decreases. If an equivalent elastic approach is being adopted to estimate settlement at the serviceability load level, then at typical safety factors for shallow foundations of 2 to 3, R_E is found to be between about 0.2 and 0.3, so that approximately within this range, R_E = 0.1FS. This is consistent with Haberfield (2013) who found that a reduction factor of 0.2 was relevant.

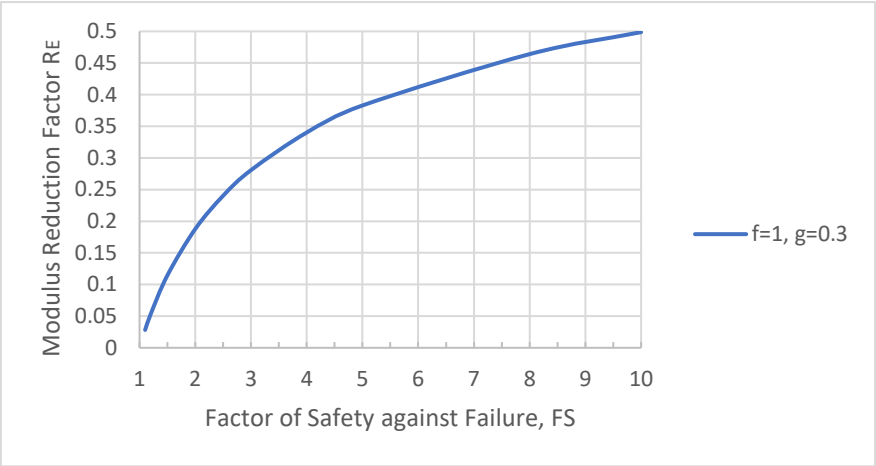

Figure 14: Modulus reduction factor RE versus Factor of Safety FS for pile foundations

APPLICATION TO THE BURJ KHALIFA TEST PILES

The foundation design for the Burj Dubai (re-named the Burj Khalifa at its opening) was described by Poulos and Bunce (2008). The ground investigation was quite comprehensive and included geophysical testing to measure P-wave and S-wave velocity profiles with depth. The ground conditions consisted of an upper layer of uncemented calcareous sand overlying various layers of cemented calcareous sediments. The general ground conditions can be characterized as being soft rock.

Figure 15 shows representative measured V_s and V_p profiles, and also a V_p profile derived from the S-wave profile, adopting a Poisson's ratio of 0.3 in equation 5. The derived values of V_p are reasonably consistent with the measured values, indicating that for geotechnical parameter correlations, V_p may be estimated from V_s measurements if direct measurements of V_p are not available, and vice-versa.

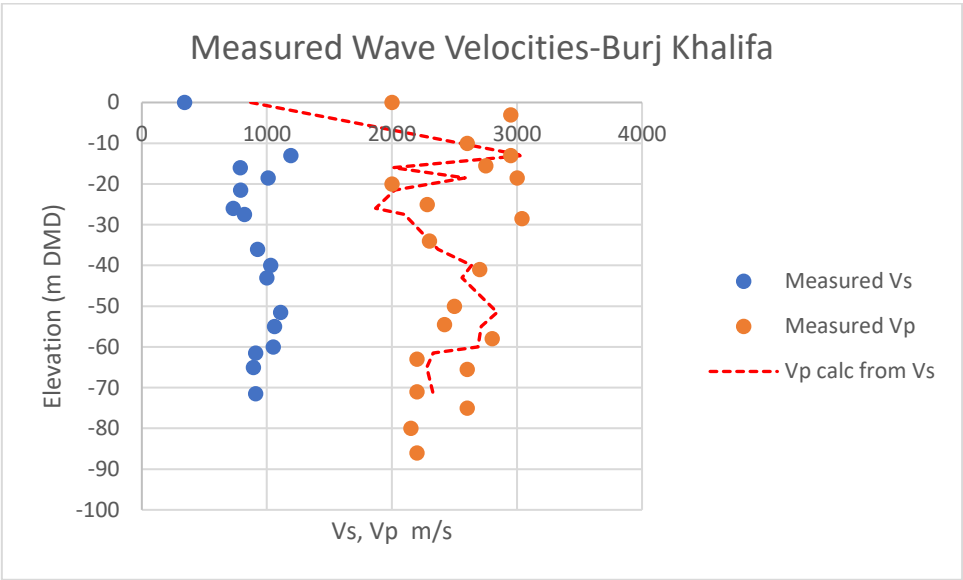

Figure 15: Comparison of measured and derived values of V_p for Burj Khalifa

As part of the foundation design, a series of pile load tests was carried out to try and verify the pile design parameters, and the details of the five compression load tests are summarized in Table 8.

Table 8: Summary of compression pile load tests for Burj Khalifa

Pile Number	*Diameter m*	*Cut-off level (m DMD)*	*Toe level (M DMD)*	*Pile length m*	*Notes*
TP-1	1.5	-4.85	-50	45.15	-
TP-2	1.5	-4.85	-60	55.15	-
TP-3	1.5	-4.85	-40	35.15	Shaft grouted
TP-4	0.9	-2.90	-50	47.10	Cyclic test
TP-5	0.9	-2.95	-50	47.05	-

The following procedure has been adopted to calculate the load-settlement behaviour of these test piles:

1. The measured shear wave velocities shown in Figure 15 have been used to estimate the small-strain Young's modulus values, E_0, from equation 7, assuming a Poisson's ratio of 0.25.
2. The unconfined compression strength (UCS) with depth has been estimated, using the Poulos correlation shown in Figure 3.
3. The ultimate shaft friction and end bearing values have been estimated from equations 22 and 23, using the recommended values of the empirical parameters A3, A4, A5 and A6.
4. The ultimate axial capacity, P_u, has then been computed for each pile by summation of the ultimate shaft and base capacities.
5. Manoj et al (2020) have found that the value of A3 of 0.3 is very conservative for a nearby site in Dubai, and that a value of A3 = 0.5 appears to be more appropriate. Therefore, calculations have been carried out for both A3=0.3 and A3=0.5.
6. Elastic theory, via Randolph and Wroth (1978), has been used with the estimated values of E_0 to obtain an estimate of the initial pile head stiffness, K_0, using an average value of E_0 along the pile shaft, and the estimated small-strain Young's modulus at the pile toe.
7. For increasing values of applied load P, the pile head settlement has been computed as follows:

$$S = P/(K_0.R_E) \quad (25)$$

where R_E is the modulus reduction factor in equation 24 and Figure 14, with a safety factor of P_u/P.

Figures 16 to 20 compare the measured and calculated load-settlement curves for the five test piles. The following points are made:

1. Using A3=0.3, the calculated settlements tend to be larger than the measured values (i.e. conservative), especially at larger loads, although the agreement at lower load levels is quite good. This may indicate that the estimated ultimate load capacities may also be conservative.
2. This indication appears to be vindicated by the results of the calculations using A3=0.5, rather than 0.3. The calculated curves using A3 = 0.5 are in remarkably good agreement with the measurement, although this agreement may well be fortuitous.
3. The extent of conservatism using A3 = 0.3 appears to be greater for TP-3, the pile that has been shaft-grouted. No account was taken of this process in estimating the ultimate shaft friction.
4. No account has been taken of the possible effects of interaction between the test piles and their reaction systems. Such interaction tends to reduce the measured settlements as

compared with a “perfect” test in which there are no effects of interaction between the test pile and the reaction system (Russo et al, 2013).

Overall, the comparisons suggest that the approach adopted is capable of providing a reasonable, if slightly conservative, estimate of the load-settlement behaviour of a single axially loaded pile, on the basis of a measured profile of shear wave velocity and the correlations adopted herein. It is also clear that, while the estimated settlement at relatively low loads is largely unaffected by the ultimate capacity, at higher loads, the accuracy of the calculated load-settlement behaviour depends considerably on the estimated ultimate axial capacity of the pile.

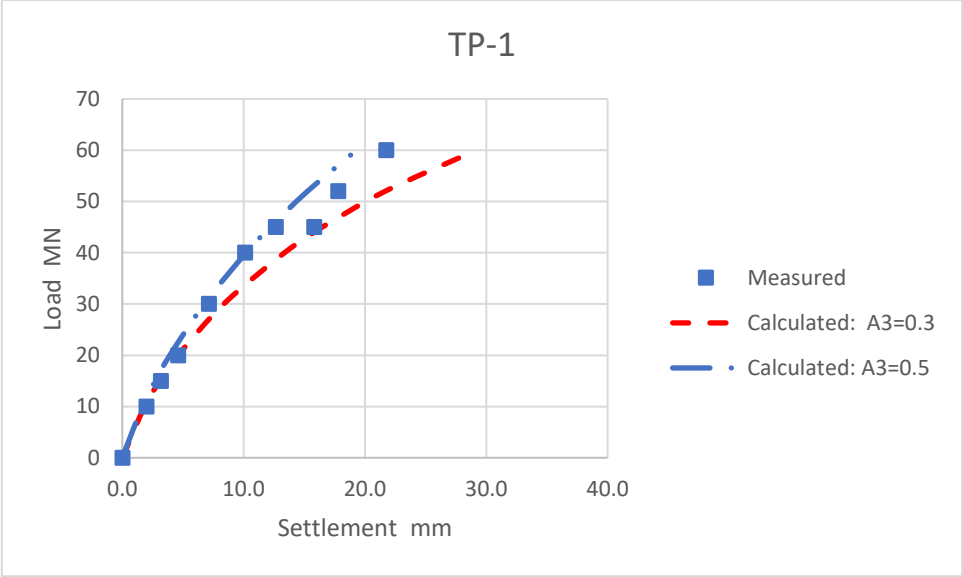

Figure 16: Measured and calculated load-settlement curves for pile TP-1

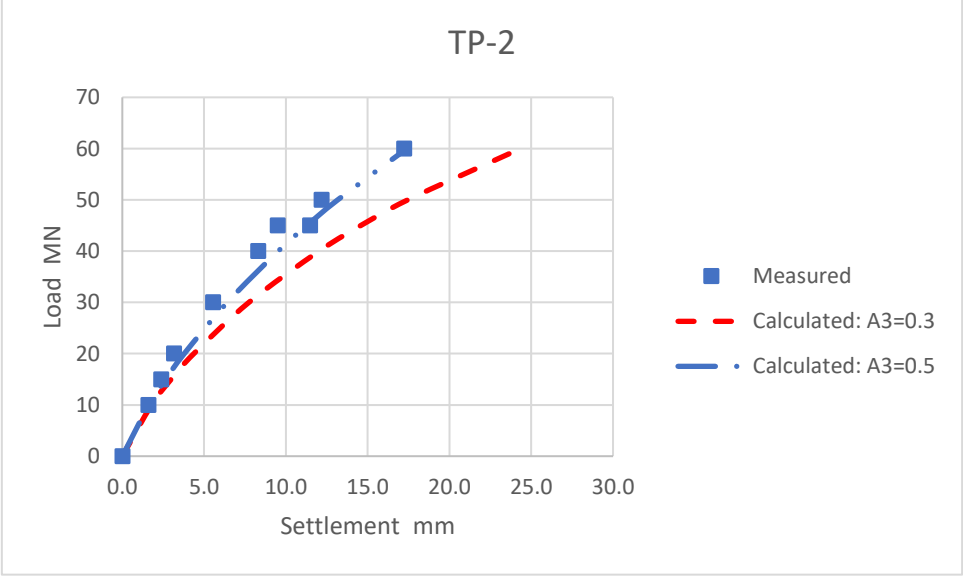

Figure 17: Measured and calculated load-settlement curves for pile TP-2

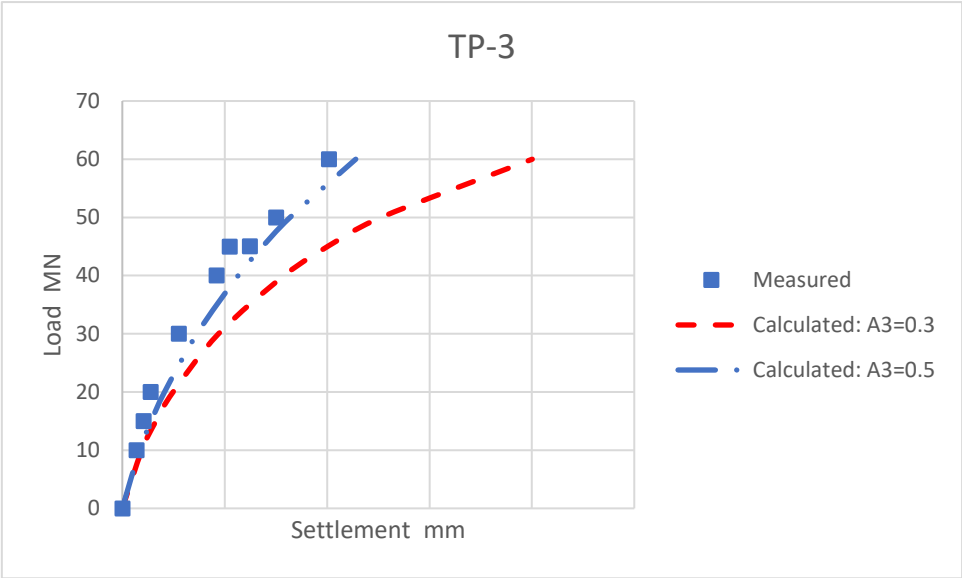

Figure 18: Measured and calculated load-settlement curves for pile TP-3

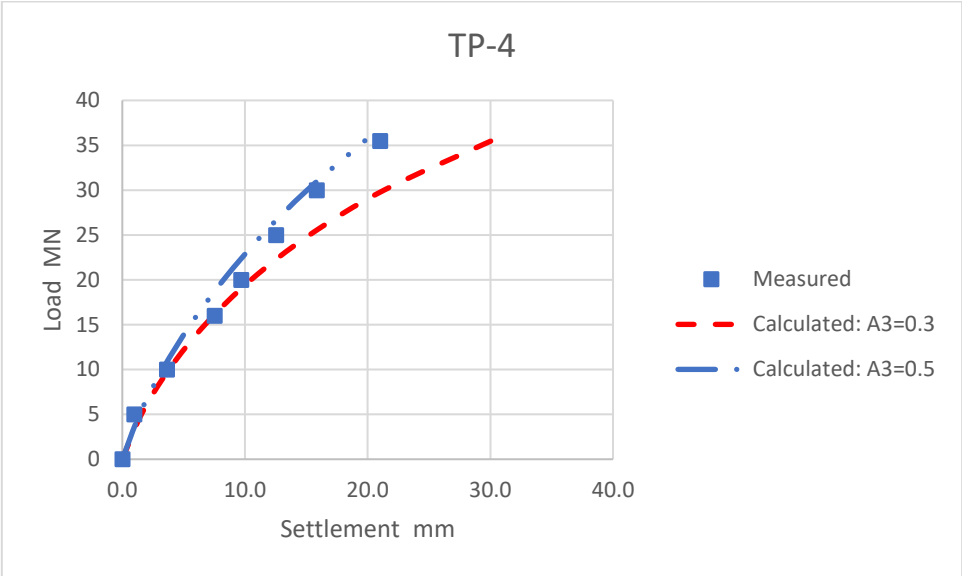

Figure 19: Measured and calculated load-settlement curves for pile TP-4

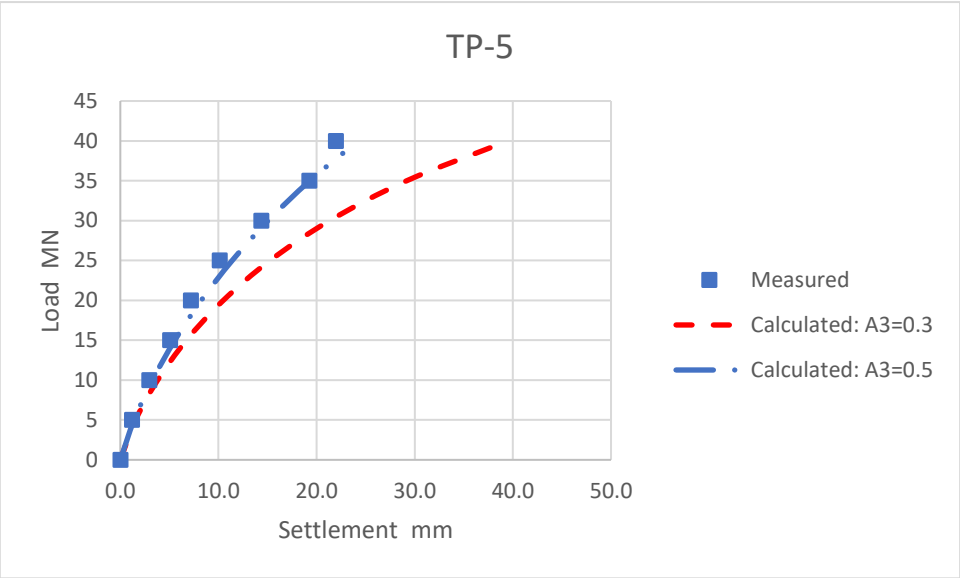

Figure 20: Measured and calculated load-settlement curves for pile TP-5

CONCLUSIONS

This paper has outlined an approach for utilizing the results of in-situ measurements of shear wave velocity V_s to estimate the load-settlement behaviour of shallow and deep foundations. V_s is used to estimate the small-strain Young's modulus of the underlying strata, and then the SPT, CPT or UCS values of these strata. Correlations can then be employed to estimate the initial foundation stiffness and the ultimate load capacity, and by use of an empirical relationship between modulus reduction and load or stress level, the settlement at various loads can be estimated.

This approach has been used to calculate the load-settlement behaviour of a series of shallow footing tests on sand, and pile load tests on soft rock. In both cases, the suggested approach provided reasonable estimates of the foundation behaviour, albeit with a tendency to be conservative. For both shallow and deep foundations both the adopted value of initial ground stiffness and the assumed ultimate resistances can have a considerable influence on the computed load-settlement behaviour.

It is emphasized that the approach described herein is not meant to be a primary design method, but rather another means of carrying out preliminary estimates of load-settlement behaviour, and of checking against the results of more complex design methods.

One of the virtues of shear wave velocity measurements is that the effects of local anomalies within the ground profile (for example, weathered zones, dykes and faults) are reflected in the measured V_s values, thus reducing or removing the need to try and estimate the mass modulus values from test results on small volumes or samples of the ground.

ACKNOWLEDGEMENTS

The author gratefully acknowledges the support of Tetra Tech Coffey in compiling this paper, and the constructive comments of his colleagues, Simon Stewart, Ross Best and Patrick Wong.

REFERENCES

Agaiby, S. and Mayne, P.W (2015). "Relationship between undrained shear strength and shear wave velocity for clays". 15th Panamerican Conference on Soil Mechs and Geot Eng, Buenos Aires, Argentina, DOI: 10.3233/978-1-61499-601-9-358

Altindag, R. (2012). “Correlation between P-wave velocity and some mechanical properties for sedimentary rocks”. Jnl. South African Inst. Min. & Metallurgy, Vol. 112: 229-237.

Azimian, A., Ajalloeian, R. and Fatehi, L. (2014). “An empirical correlation of uniaxial compressive strength with P-wave velocity and point load strength index on marly rocks using statistical method”. Geotech. Geol. Eng. 32: 205-214.

Briaud, J-L. and Gibbens, R.M. (1994). “Predicted and measured behavior of five spread footings on sand”. ASCE Geot. Special Publication No. 41.

Cha, M. Santamarina, C., Kim, H-S. and Cho, G-C. (2014). “Small-strain stiffness, shear-wave velocity, and soil compressibility”. J. Geotech. Geoenviron. Eng., ASCE, 06014011-1 to 4.

Cheenikal, L., Poulos, H. and Whiteley, R. (2007). “Geophysical testing for rock assessment and pile design”. Proc. 10th Australia - New Zealand Conf. Geomechanics, Brisbane, 442-447.

Decourt, L. (1995). “Prediction of load-settlement relationships for foundations on the basis of the SPT-T”. Ciclo de Conferencias International “Leonardo Zeevaert, UNAM, Mexico, pp 85-104.

Fahey, M. and Carter, J.P. (1993). “A finite element study of the pressuremeter using nonlinear elastic plastic model”. Can Geot. Jnl., 30(2): 348-362.

Haberfield, C.M.(2013). “Tall tower foundations - from concept to construction”. In K.K. Phoon et al (eds), Advances in Foundation Engineering. Research Publishing Services, Singapore, pp 33-65.

Hegazy, Y.A. and Mayne,P.W. (1995). “Statistical correlations between Vs and cone penetration test data for different soil types”. Proceedings, International Symposium on Cone Penetration Testing, CPT’ 95, Linköping, Sweden, Vol. 2, 173-178.

Hyder (2004). “Burj Dubai Development, Dubai UAE. Works pile testing report”. Report GD00631/GDR/2004/01, prepared for Emaar Properties.

Garfield,R. and Reid, J. (2021). “DFI145 Panel: advancing geophysics use in subsurface characterization”. Deep Foundations, DFI, Jan/Feb 2021, 75-78.

Godlewski, T. and Szczezepanski, T. (2015). “Measurement of soil shear wave velocity using in situ and laboratory seismic methods – some methodological aspects”. Geol. Quarterly, 59(2): 358-366.

Imai, T. and Tonouchi, K. (1982). “Correlation of N-value with S-wave velocity and shear modulus,” Proc. 2nd European Symp. Of Penetration Testing (Amsterdam), 57–72.

JRA (Japan Road Association) (1980). “Specification and interpretation of bridge design for highway-part V: Resilient design.

L’Heureux, J.S. and Long, M. (2017). “Correlations between shear wave velocity and geotechnical parameters in Norwegian clays”. J. Geotech. Geoenvir. Eng., ASCE, 04017013-1 to 20.

Majstorovic, J., Gligoric, M., Lutovac, S. Negovanovic, M. and Crnogorac, L. (2019). “Correlation of uniaxial compressive strength with the dynamic elastic modulus, P-wave velocity and S-wave velocity of different rock types. Underground Mining Engineering, Univ of Belgrade, 11-25.

Manoj, S., Choudhary, D. and Alzaylaie, M. (2020). "Value engineering using load-cell test data of barrette foundations – La Maison, Dubai". Proc. Instn. Civil Engrs.– Geotechnical Engineering, https://doi.org/10.1680/geen.19.00246.

Mayne, P.W. (2001). "Stress-strain-strength-flow parameters from enhanced in-situ tests". In P.P. Rahadjo and T. Lunne (Eds), Proc. Int. Conf. on In-Situ Measurement of Soil Properties and Case Histories, Bali, Indonesia, pp 27-48.

MELT (1993). "Regles techniques de conception et de calcul des fondations des ouvrages de genie civil". Cahier des Clauses Techniques Generales applicables aux Marches Publics de Travaux, Fascicule 62 – Titre V. Ministere de L'Equipment du Logement st des Transports, Paris.

Niazi, F.S. and Mayne, P.W. (2013). "A review of the design formulations for static axial response of deep foundations from CPT data". DFI Journal, 7(2): 58-78.

Ohta, Y., Goto, N., Kagami, H. and Shiono, K. (1978). "Shear wave velocity measurement during a Standard Penetration Test". Earthquake Eng. and Structural Dynamics, 6: 43-50.

Poulos, H.G. (2017). "Tall building foundation design". CRC Press, Boca Raton, FL. USA.

Poulos, H.G. and Bunce, G. (2008). "Foundation design for the Burj Dubai – the world's tallest building".

Randolph, M.F. and Wroth, C.P. (1978). "Analysis of deformations of vertically loaded piles". Jnl Geot Eng Divn., ASCE, 104(GT12): 1465-1488.

Russo, G., Abagnara, V., Poulos, H.G. and Small, J.C. (2013). "Re-assessment of foundation settlements for the Burj Khalifa, Dubai". Acta Geotechnica, 8(1): 3-15.

Seed, H.B., Idriss, I.M. and Arango, I. (1983). "Evaluation of liquefaction potential using field performance data". J. Geot. Eng. ASCE, 124(5): 458-482.

Wair, B.R., DeJong, J.T. and Shantz, T. (2012). "Guidelines for estimation of shear wave velocity profiles". Pacific Earthquake Eng. Res. Center, PEER Report 2012/08, Univ. California.

DECLARATIONS

Funding: Not applicable. Author's own time.

Data Availability: Available on request

Conflict of Interest: None

Code availability: Not applicable

Figures

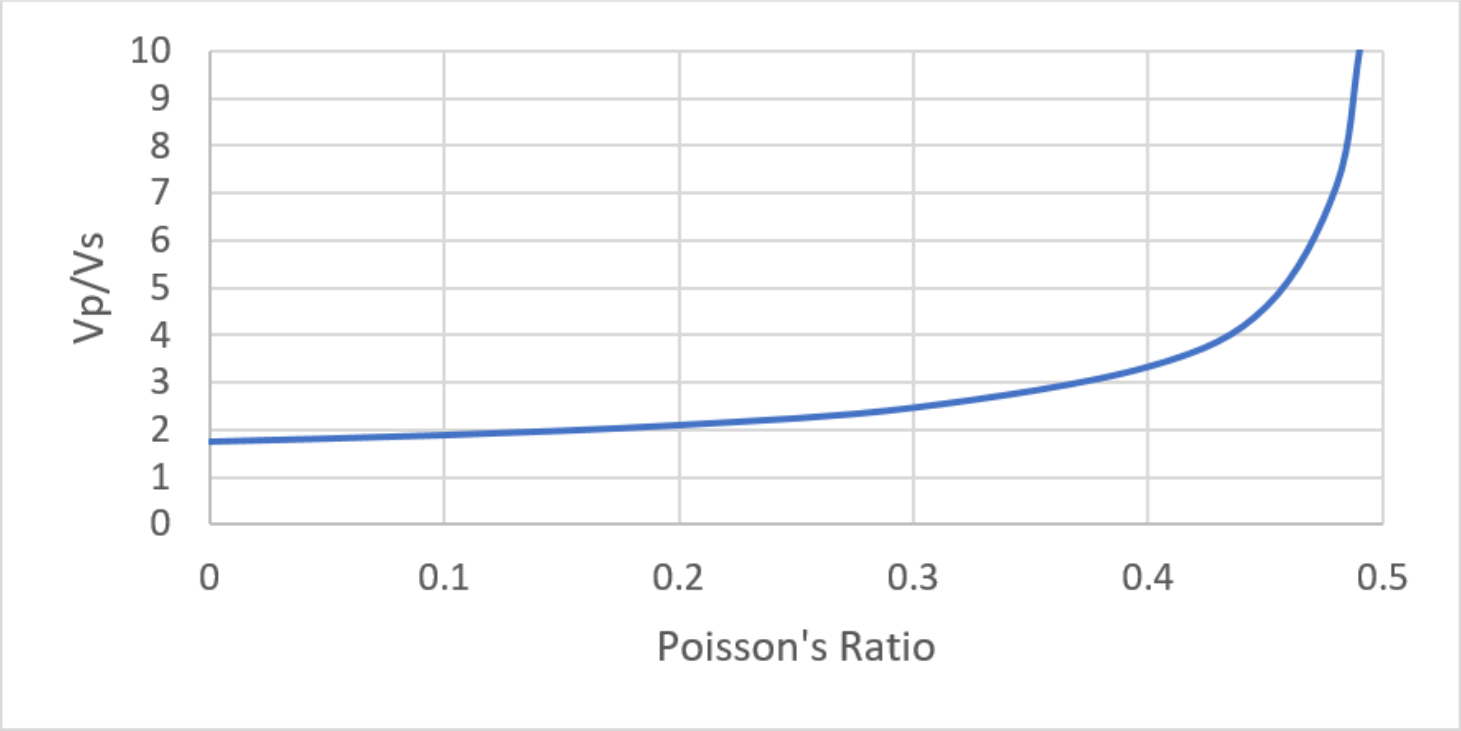

Figure 1

Theoretical relationship between Vp/Vs and Poisson's ratio v

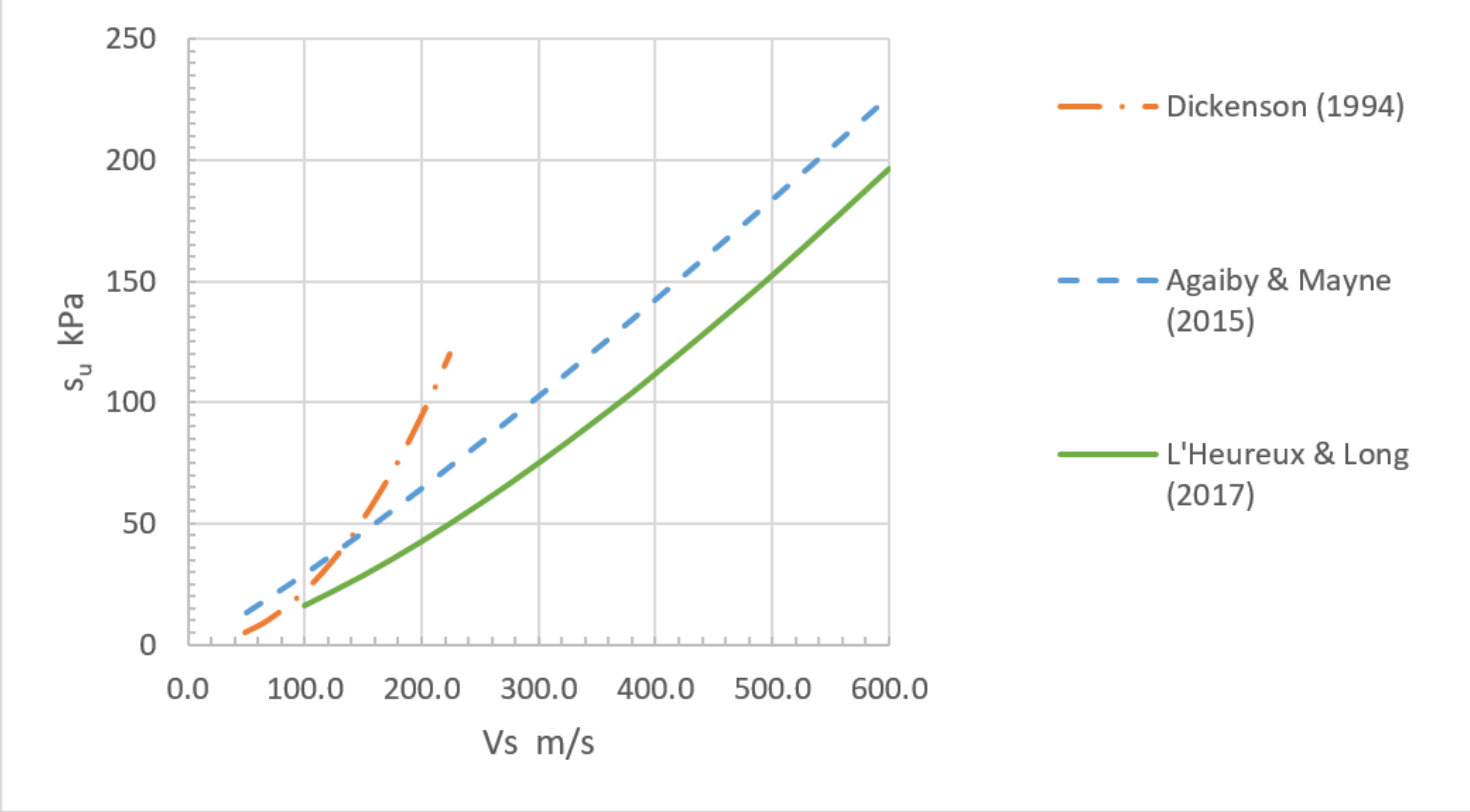

Figure 2

Correlations of su versus Vs

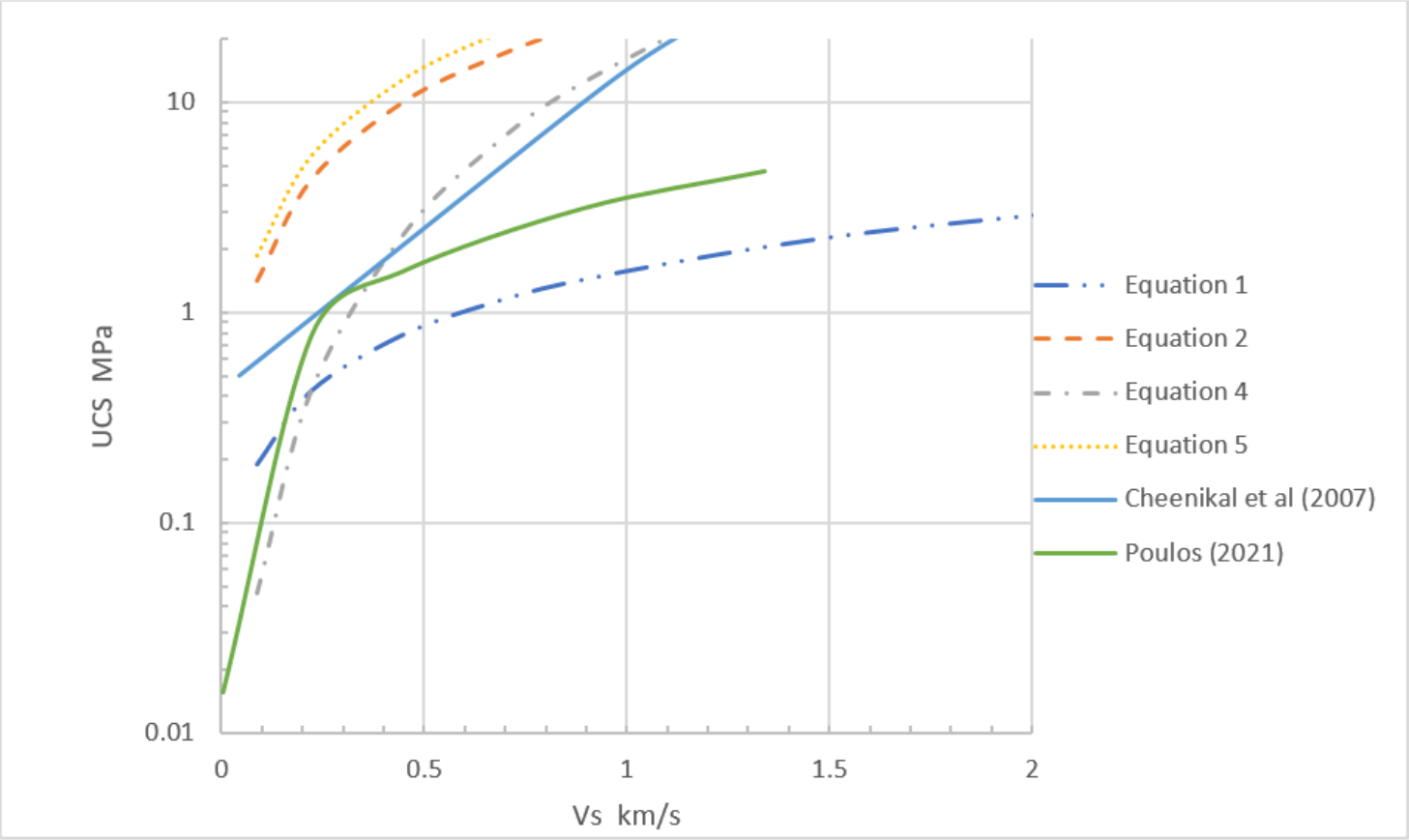

Figure 3

Some relationship between UCS and Vs (Vs derived from Vp)

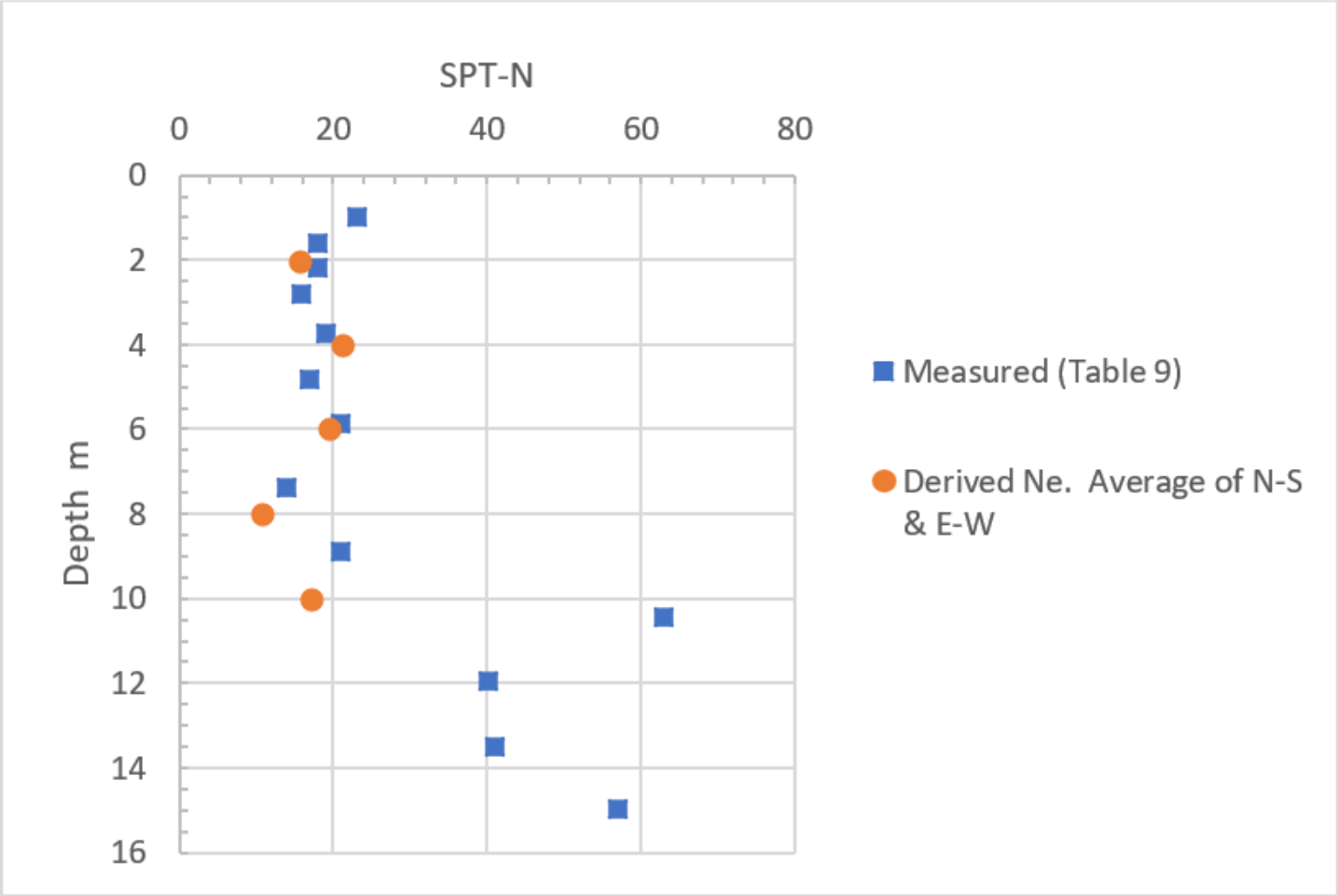

Figure 4

Modulus reduction factors for a shallow circular footing. z = depth below surface, d = equivalent footing diameter, p/pu = average pressure divided by ultimate value, E/Eo = modulus relative to small-strain value.

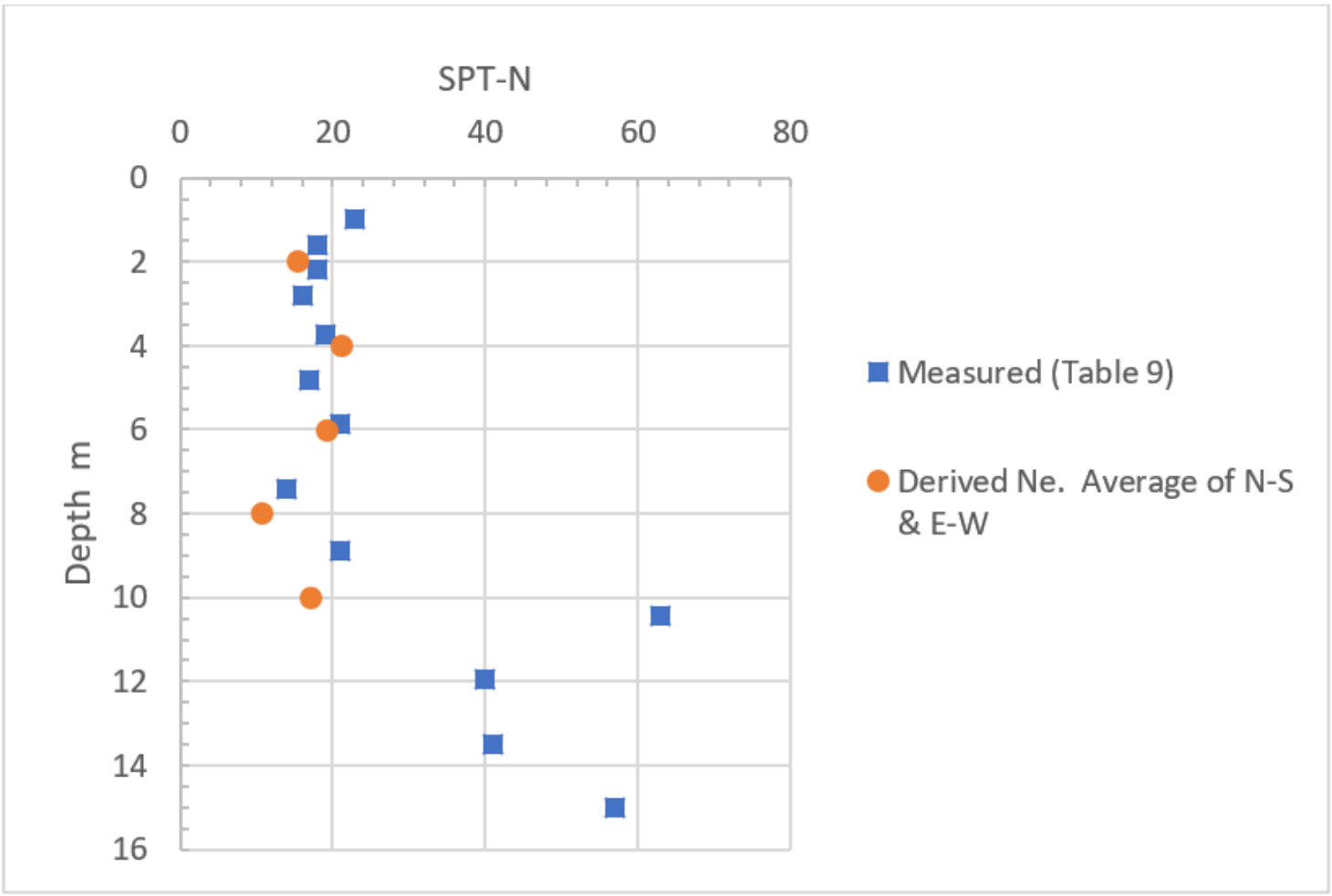

Figure 5

Comparison between measured and derived SPT values

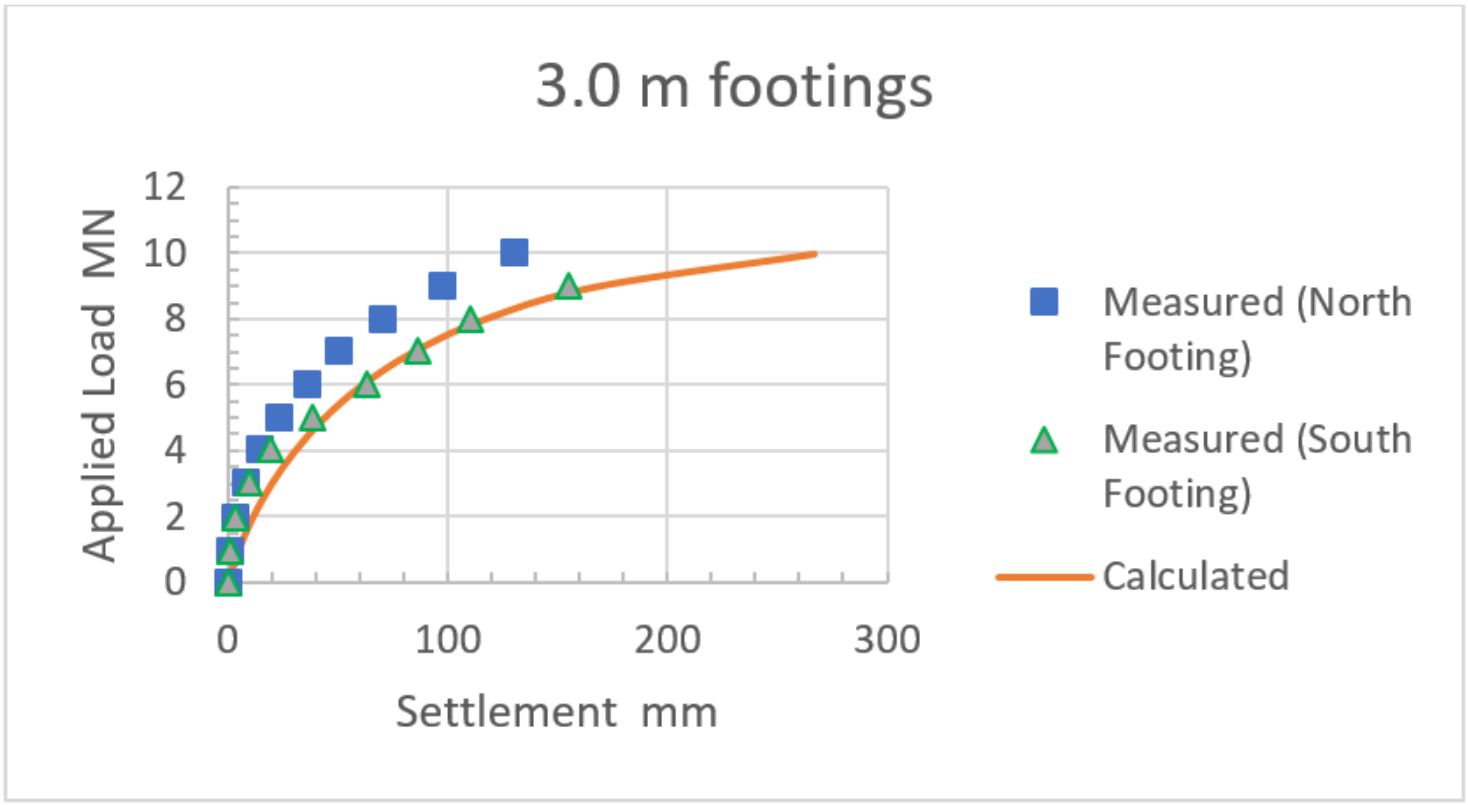

Figure 6

Measured and calculated load-settlement curves for 3 m diameter footings

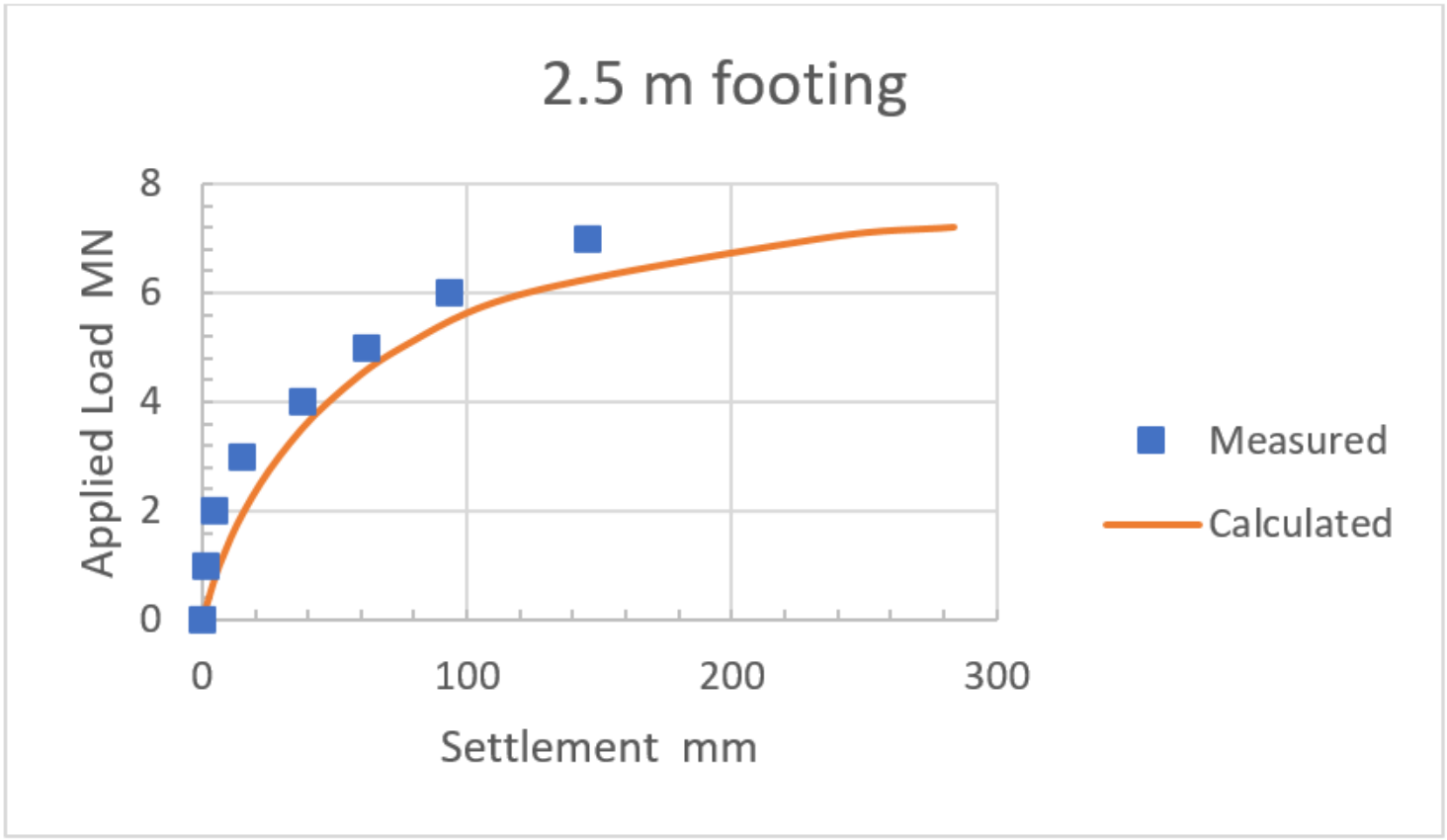

Figure 7

Measured and calculated load-settlement curves for 2.5 m diameter footing

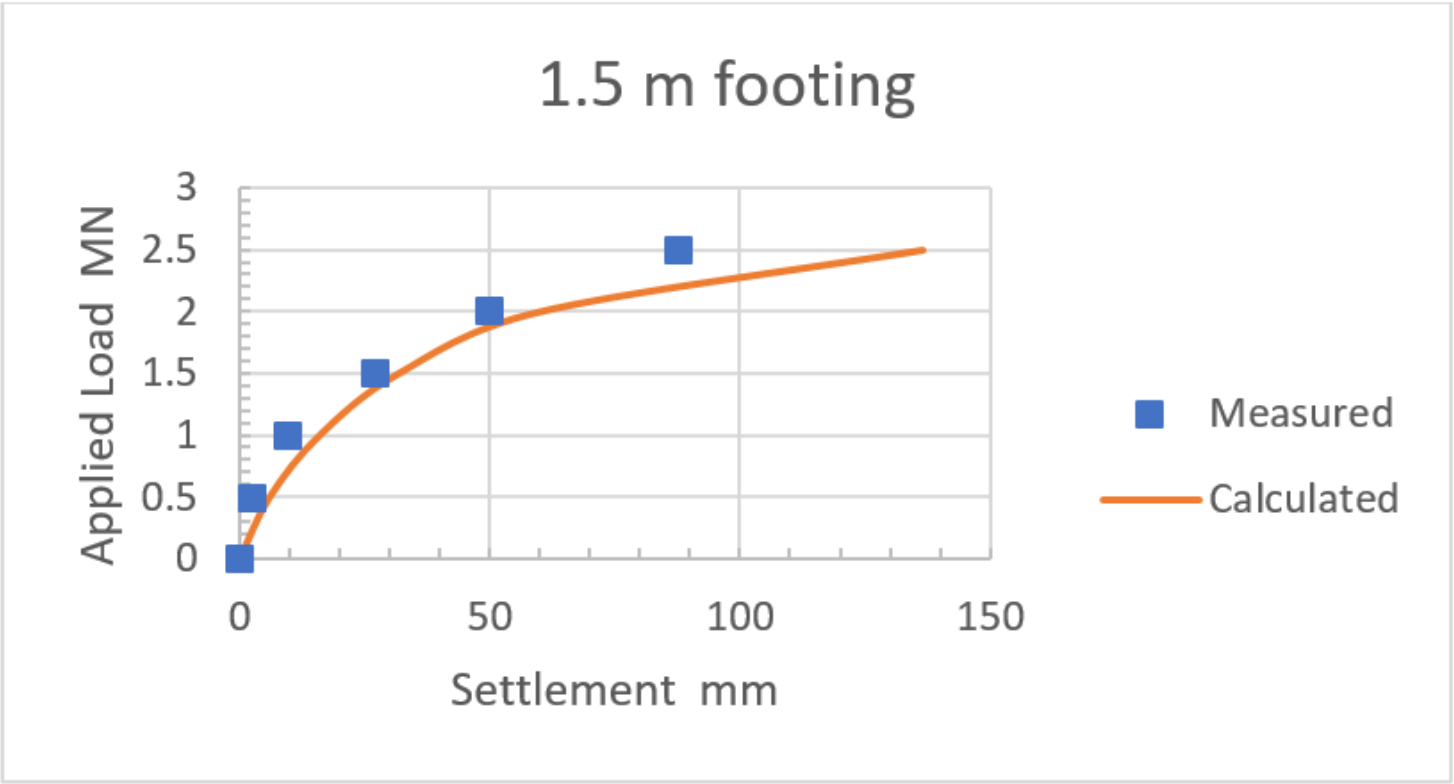

Figure 8

Measured and calculated load-settlement curves for 1.5 m diameter footing

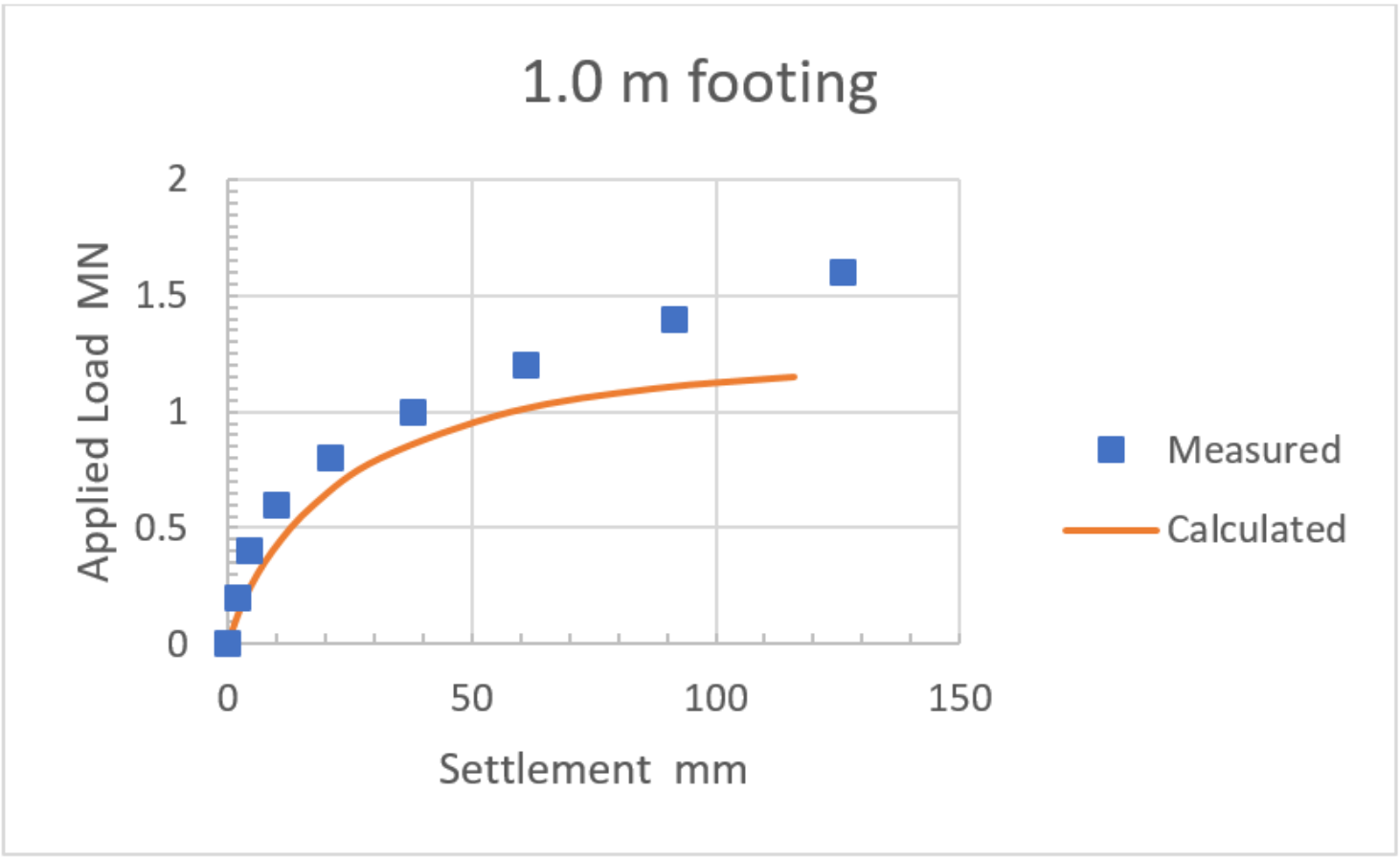

Figure 9

Measured and calculated load-settlement curves for 1 m diameter footing

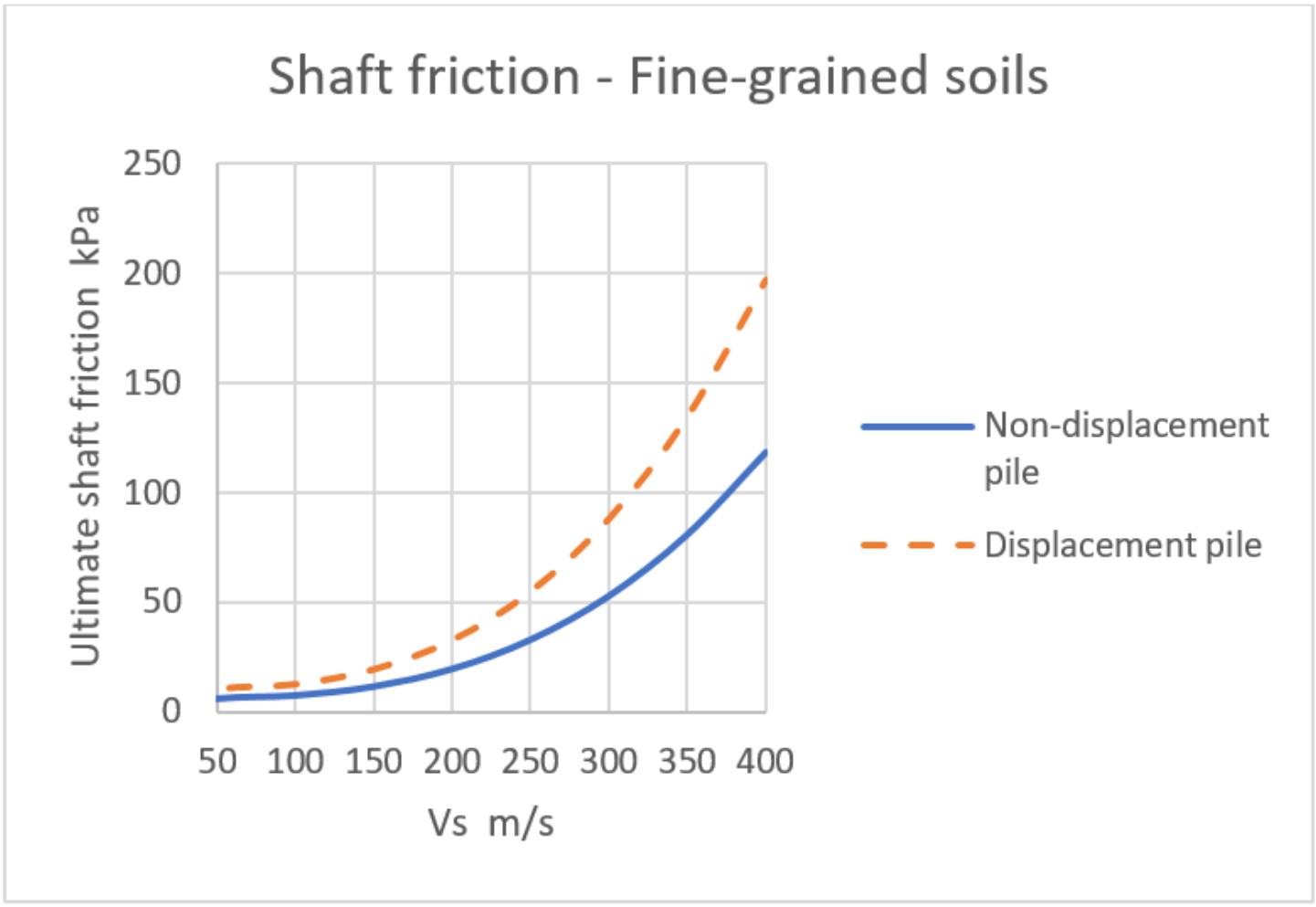

Figure 10

Approximate correlations between ultimate shaft friction and Vs for fine-grained soils

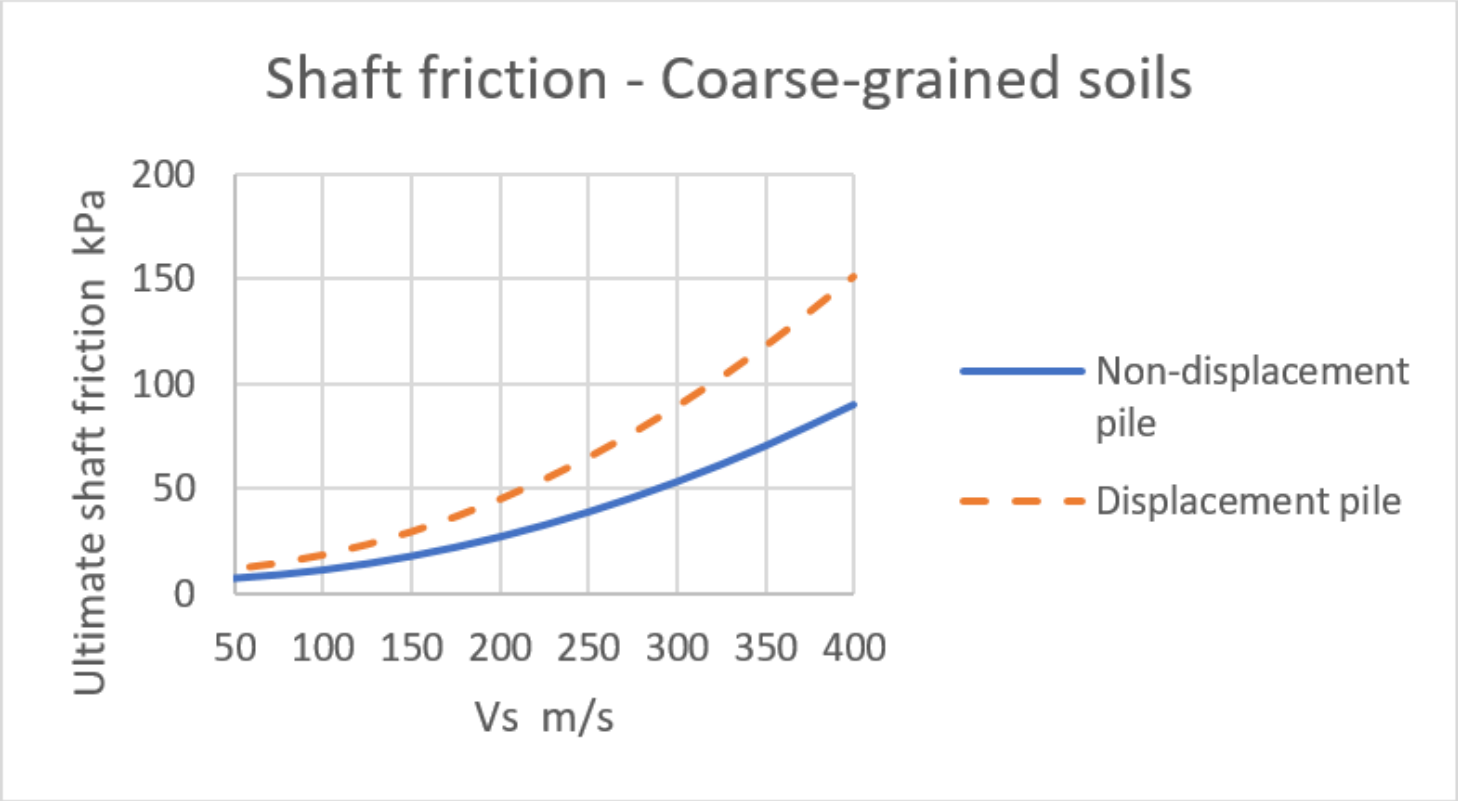

Figure 11

Approximate correlations between ultimate shaft friction and Vs for coarse-grained soils

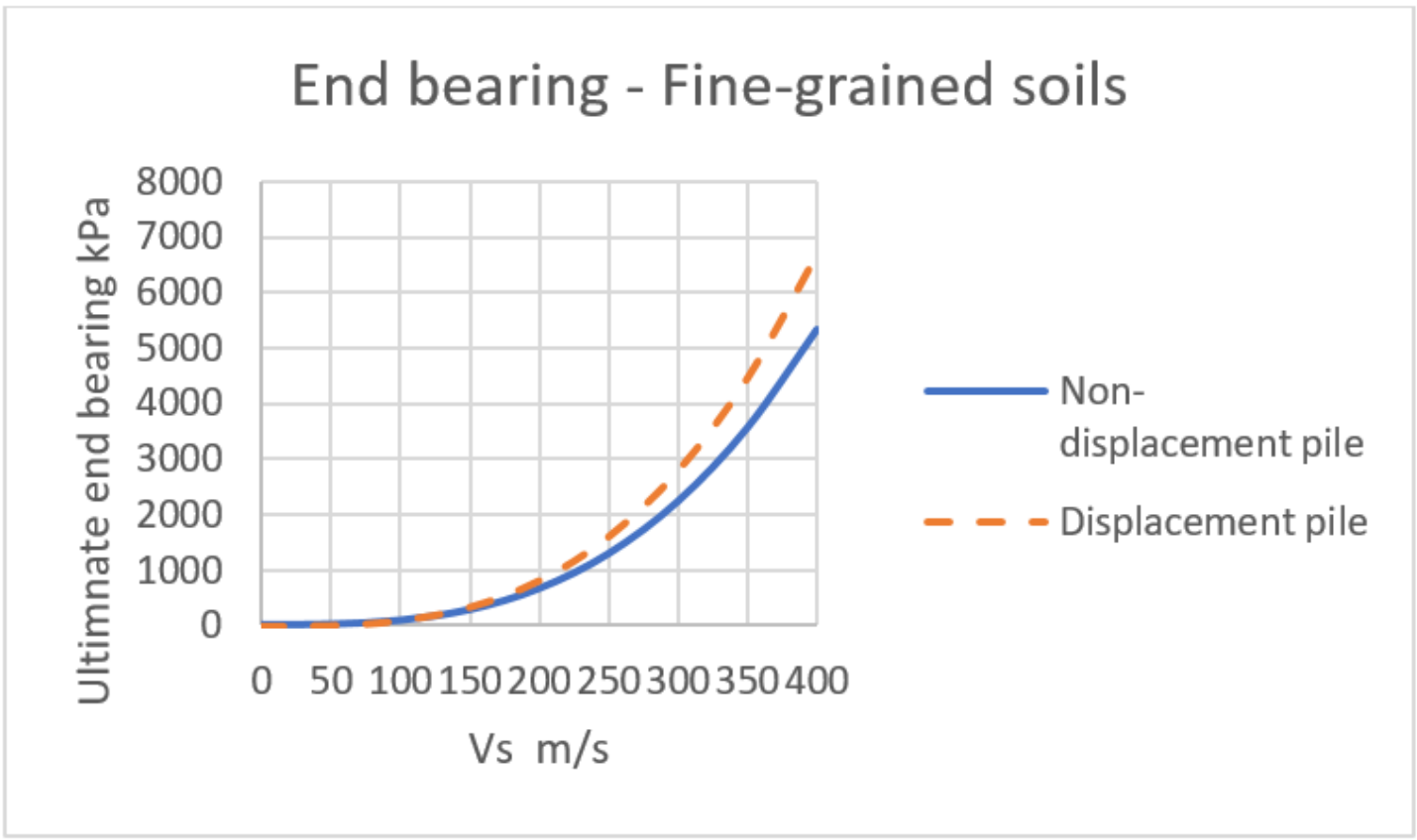

Figure 12

Approximate correlations between ultimate end bearing and Vs for fine-grained soils

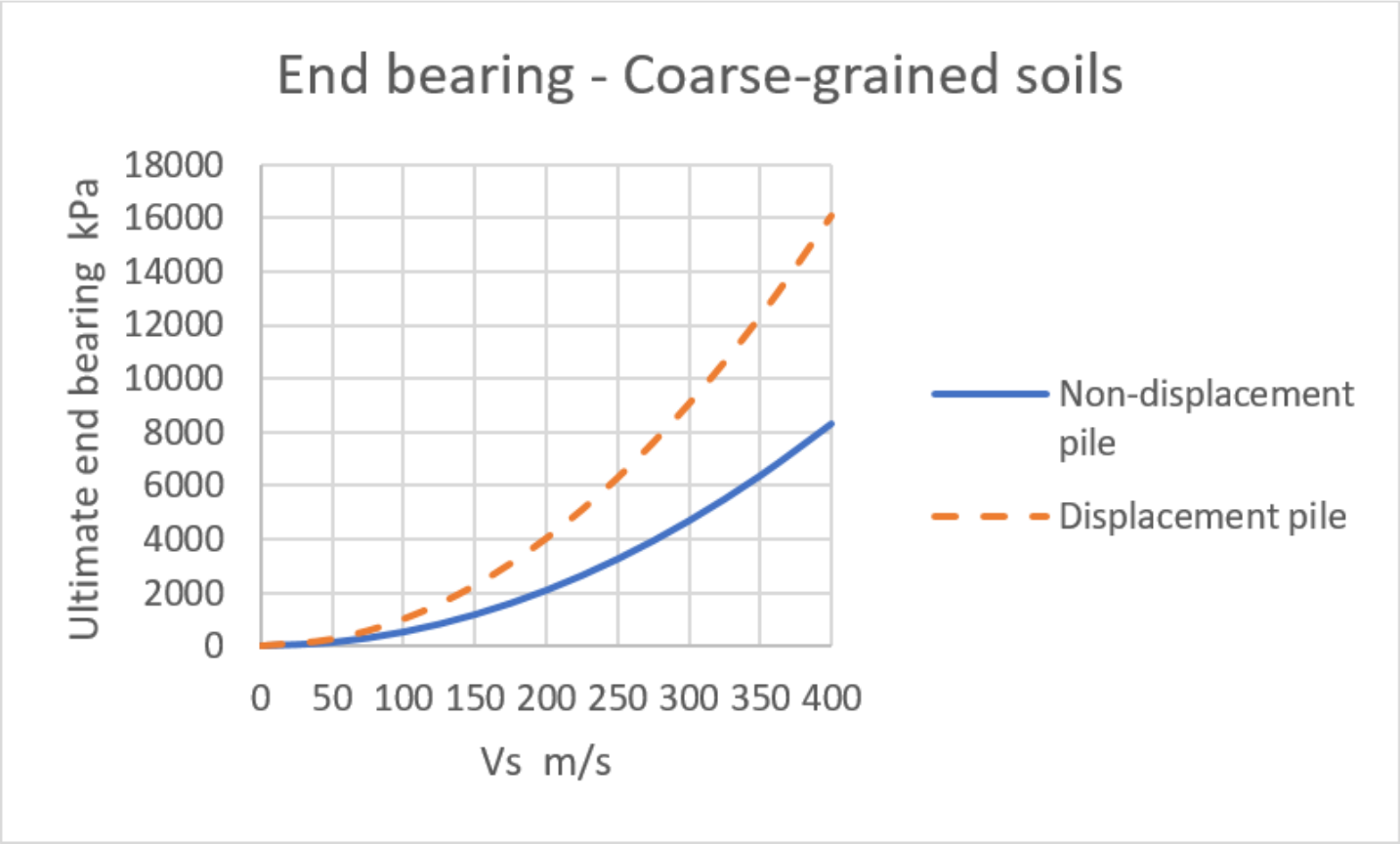

Figure 13

Approximate correlations between ultimate end bearing and Vs for coarse-grained soils

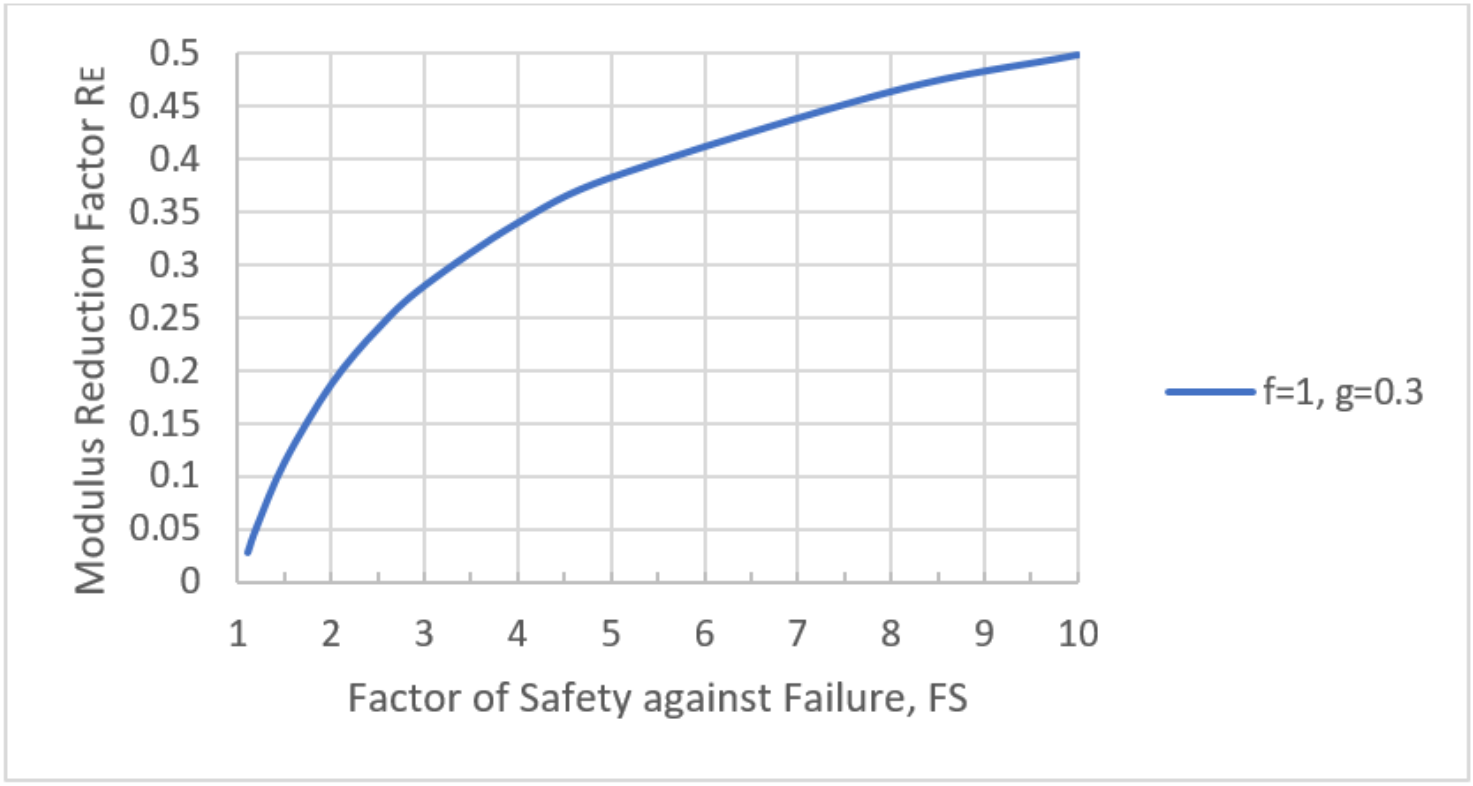

Figure 14

Modulus reduction factor RE versus Factor of Safety FS for pile foundations

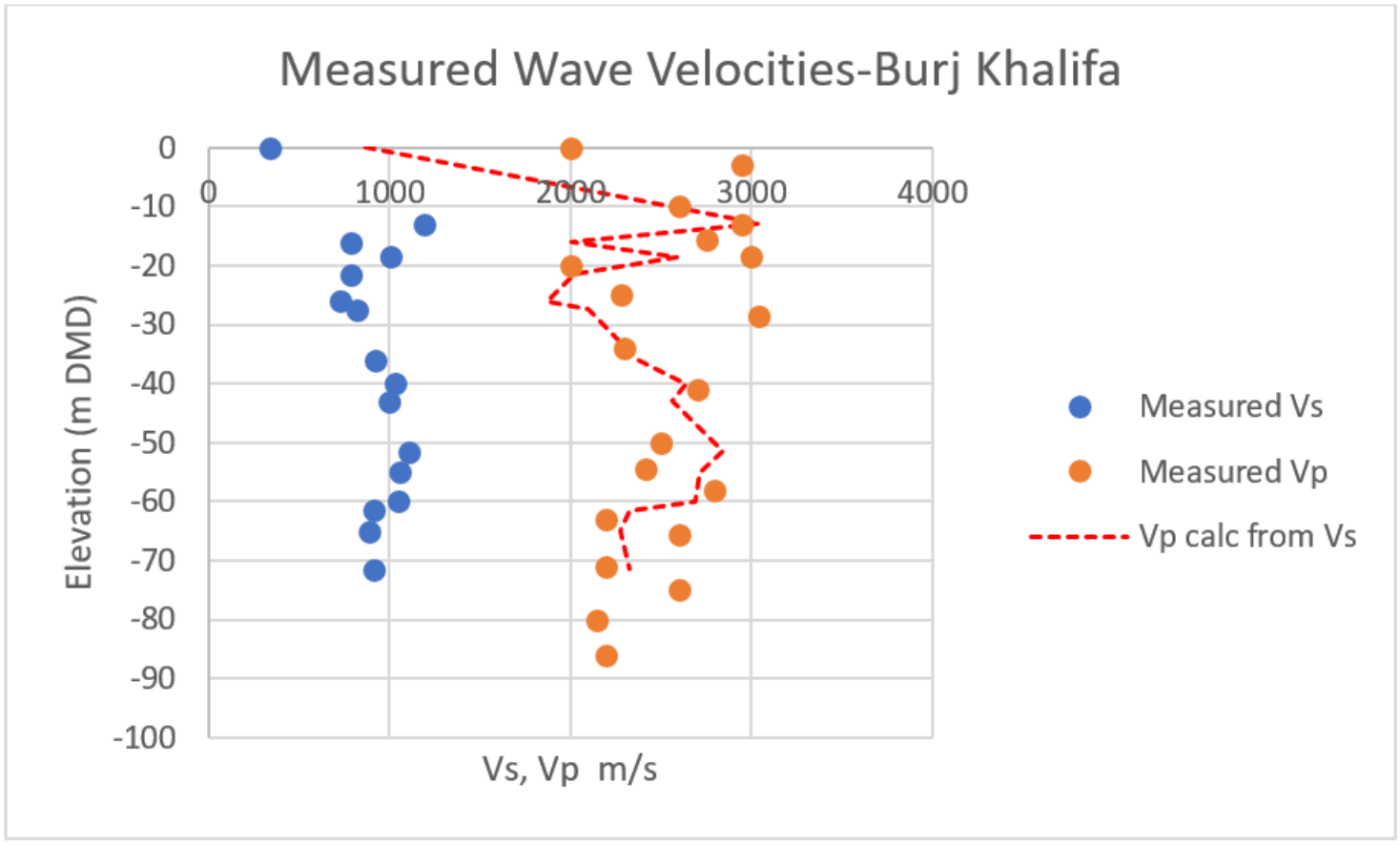

Figure 15

Comparison of measured and derived values of Vp for Burj Khalifa

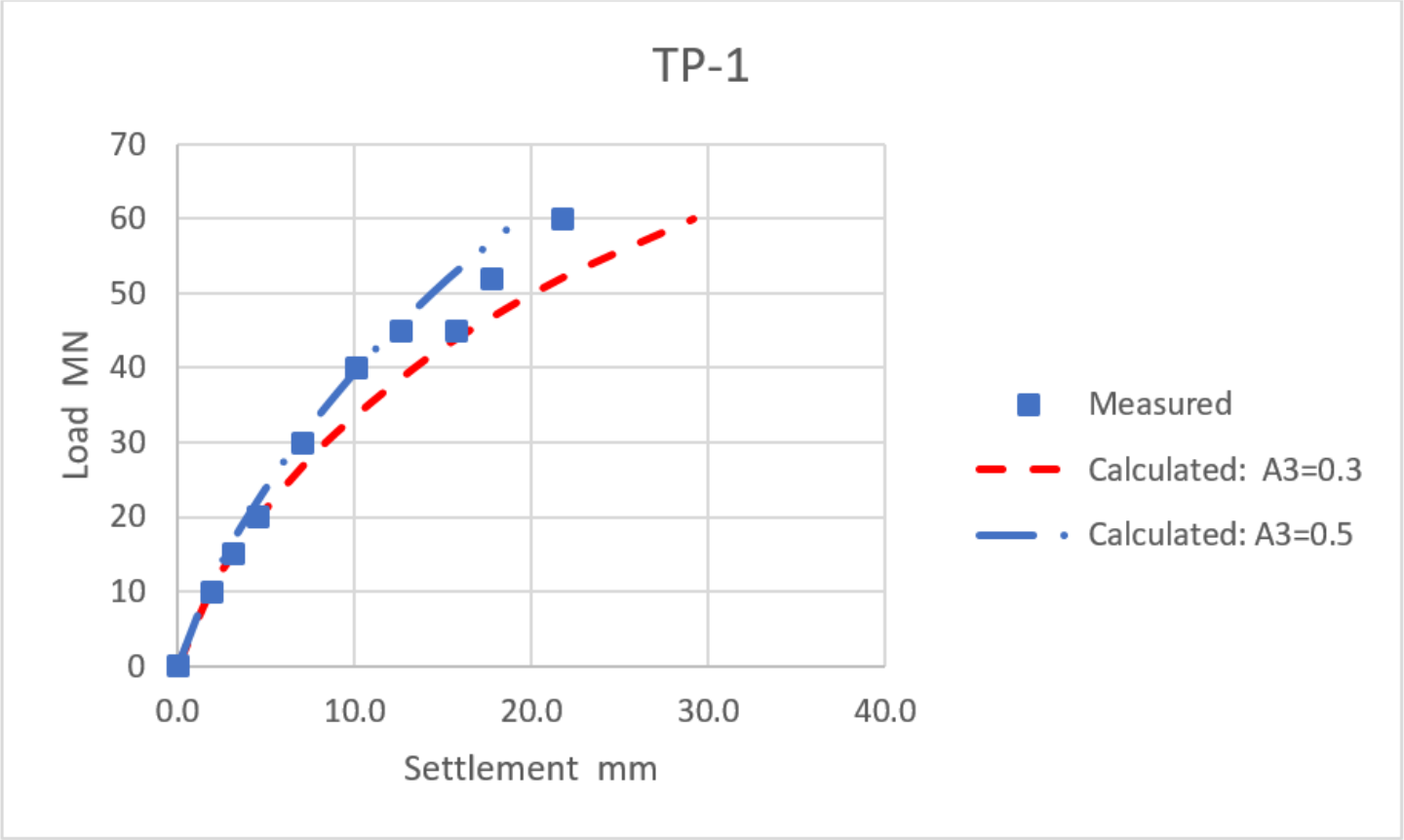

Figure 16

Measured and calculated load-settlement curves for pile TP-1

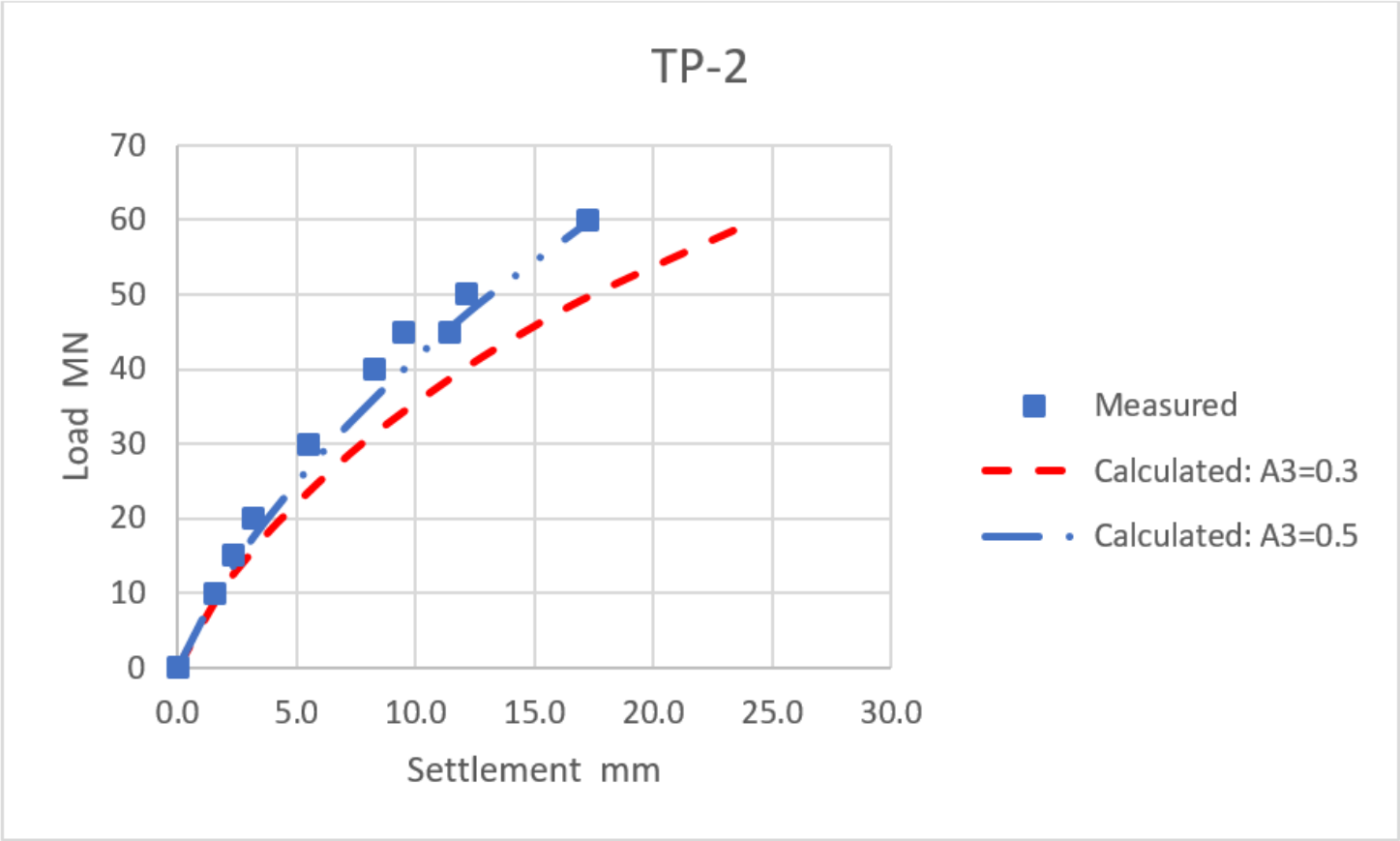

Figure 17

Measured and calculated load-settlement curves for pile TP-2

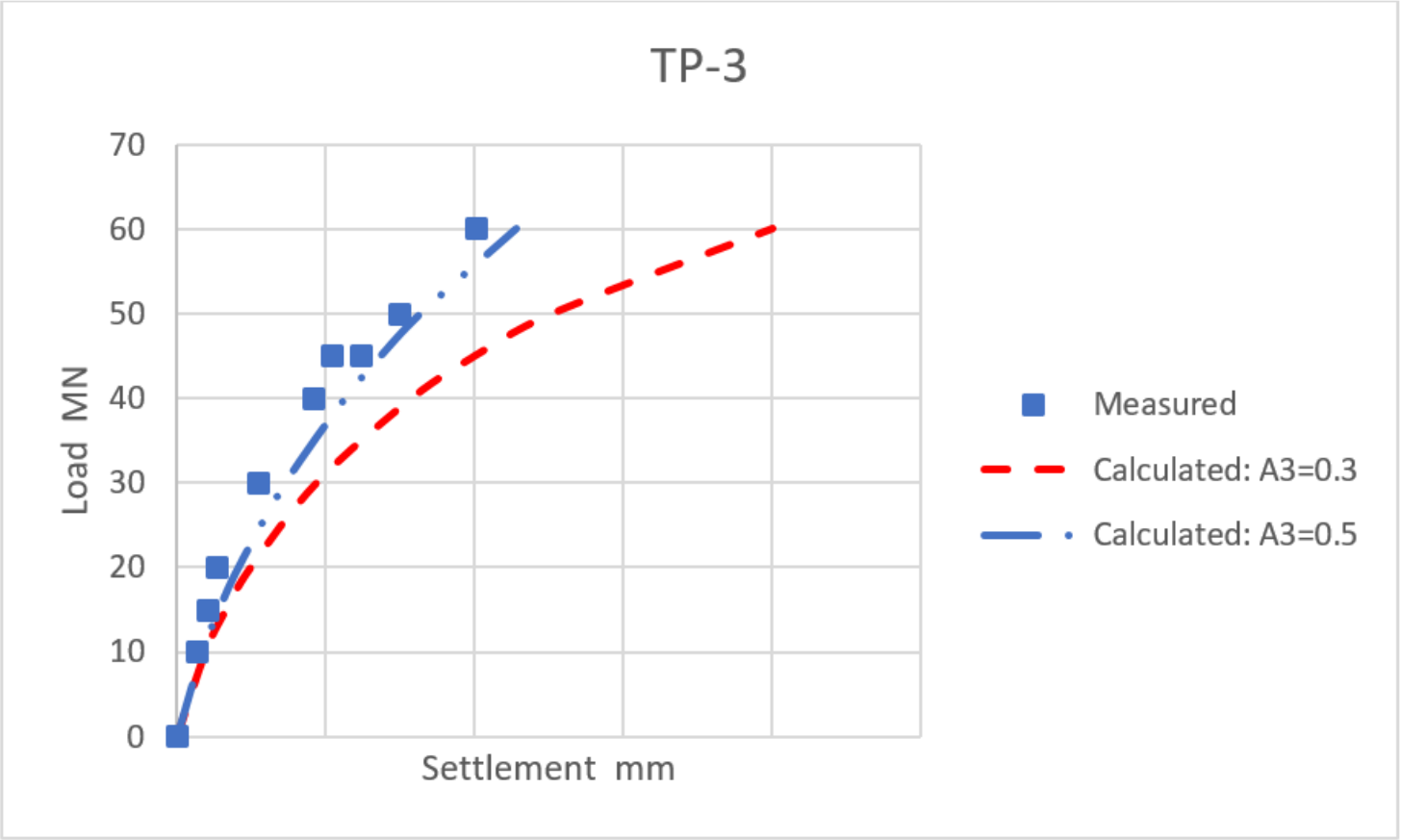

Figure 18

Measured and calculated load-settlement curves for pile TP-3

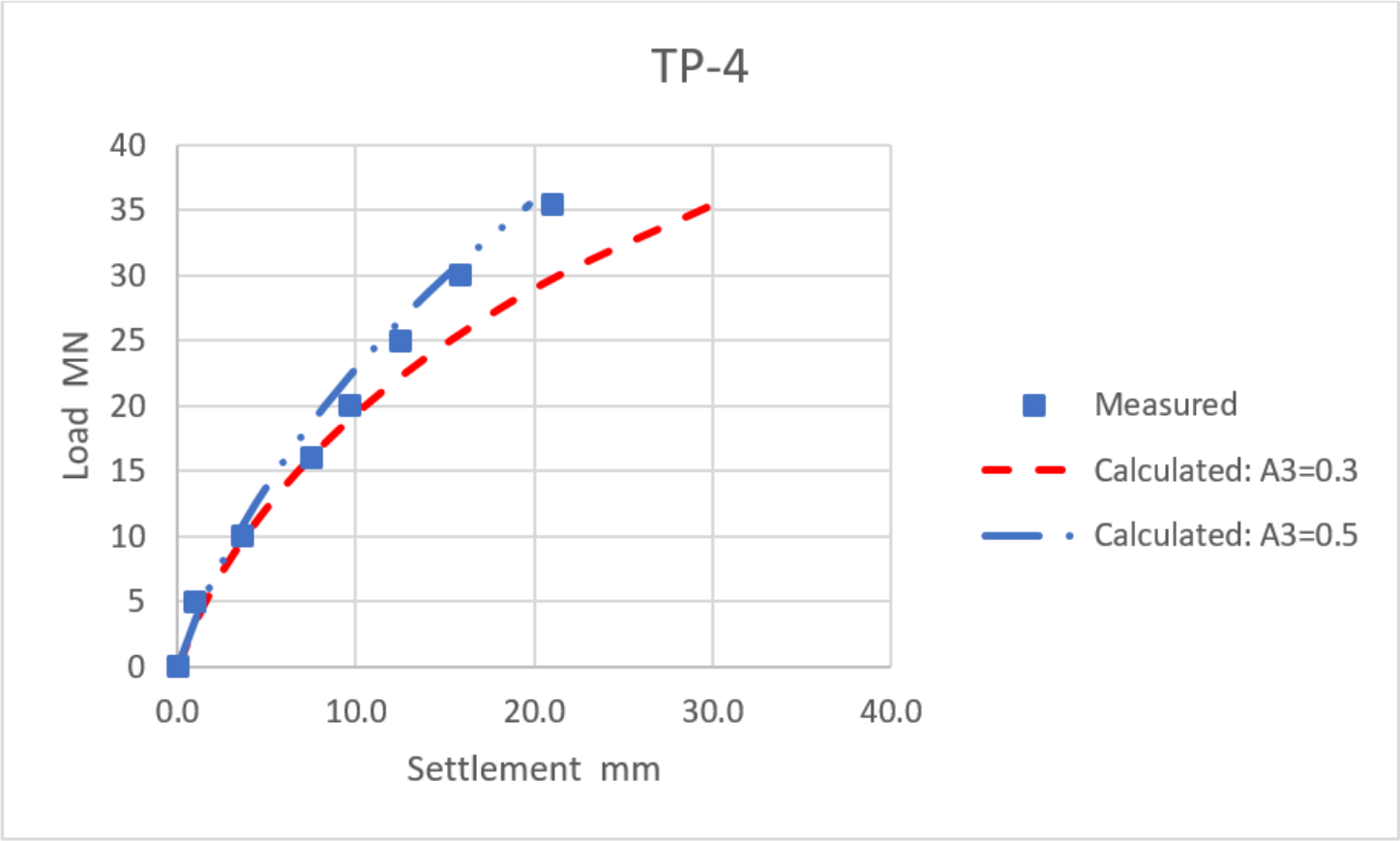

Figure 19

Measured and calculated load-settlement curves for pile TP-4

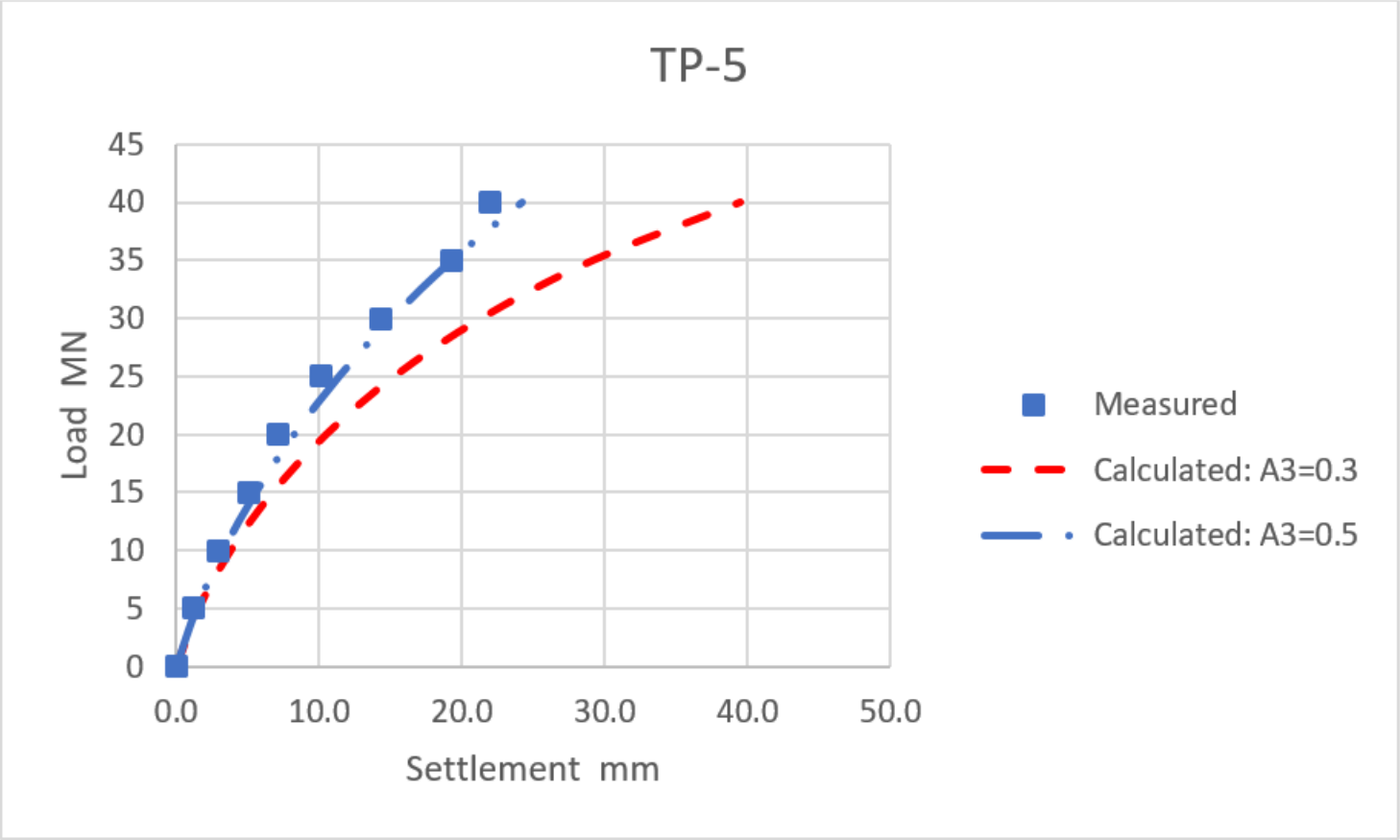

Figure 20

Measured and calculated load-settlement curves for pile TP-5